Journal of Biotechnology 309 (2020) 113–130

Contents lists available at ScienceDirect

Journal of Biotechnology

journal homepage: www.elsevier.com/locate/jbiotec

Interactive role of salicylic acid and nitric oxide on transcriptional reprogramming for high temperature tolerance in *lablab purpureus* L.: Structural and functional insights using computational approaches

Krishna Kumar Rai[a,b], Nagendra Rai[b], Mohd Aamir[a], Deepika Tripathi[a], Shashi Pandey Rai[a,*]

[a] Centre of Advance Study in Botany, Department of Botany, Institute of Science, Banaras Hindu University (BHU), Varanasi, 221005 Uttar Pradesh, India
[b] Indian Institute of Vegetable Research, Post Box-01, P.O.-Jakhini (Shahanshahpur), Varanasi, 221305, Uttar Pradesh, India

ARTICLE INFO

Keywords:
Salicylic acid
Nitric oxide
High temperature
Heat shock transcription factor
Homology modelling

ABSTRACT

Salicylic acid (SA) and nitric oxide (NO) are considered as putative plant growth regulators that are involved in the regulation of an array of plant's growth and developmental functions under environmental fluctuations when applied at lower concentrations. The possible involvement of NO in SA induced attenuation of high temperature (HT) induced oxidative stress in plants is however, still vague and need to be explored. Therefore, the present study aimed to investigates the biochemical and physiological changes induced by foliar spray of SA and NO combinations to ameliorate HT induced oxidative stress in *Lablab purpureus* L. Foliar application of combined SA and NO significantly improved relative water content (27.8 %), photosynthetic pigment content (67.2 %), membrane stability (45 %), proline content (1.0 %), expression of enzymatic antioxidants (7.1–18 %) along with pod yield (1.0 %). Heat Shock Factors (HSFs) play crucial roles in plants abiotic stress tolerance, however there structural and functional classifications in L. *purpureus* L. is still unknown. So, *In-silico* approach was also used for functional characterization and homology modelling of HSFs in L. *purpureus*. The experimental findings depicted that combine effect of SA and NO enhances tolerance in HT stressed L. *purpureus* L. plants by regulating physiological functions, antioxidants, expression and regulation of stress-responsive genes *via* transcriptional regulation of heat shock factor.

1. Introduction

In nature, plants are continuously exposed to an extreme range of temperatures during the main cropping season as well as during individual days (De Boeck et al., 2015) that determine their growth, development, and productivity. The current report on climate change has speculated an increase in the global mean temperature up to 3 − 6 °C by 2100 (IPCC, 2014). Therefore, among several abiotic stresses, high temperature has become the centre of attention because of its detrimental effects on plant growth. The plants sense high temperature (HT) as stress when the temperature increases beyond the optimum threshold for an extended period that limits their growth and metabolism (Bita and Gerats, 2013). At the physiological level, HT stress has severe repercussion on the plant's metabolic processes that reduces nutrient assimilation and translocation (Zandalinas et al., 2016). At the cellular level, HT induced oxidative stress results in the generation of reactive oxygen species (ROSs) which at basal level participate in signalling processes and at higher level causes cell death by provoking membrane peroxidation, protein oxidation and enzyme inhibition (Mittler, 2020).

Salicylic acid (SA) is a phenolic compound that has been long been known for improving plant abiotic stress tolerance (Miura and Tada, 2014). Exogenous application of SA either by seed soaking, foliar application or irrigation has been shown to improve the resilience of crop plants to environmental fluctuations by modulating physiological processes, production of osmolytes and induction of defence-related genes (Nazar et al., 2015; Zhang et al., 2015). Further, nitrogen monoxide or nitric oxide (NO) is an uncharged, redox signalling gaseous molecule that also play important role in the regulation of plant growth and physiology under stress conditions (Gill et al., 2013). NO is known to mitigate heat-induced oxidative stress by acting as second messenger in several physiological, cellular and molecular processes (Ticha et al., 2017).

Plant heat shock factors (HSFs) play a major role in protecting plants from abiotic stresses by modulating the expression of several signalling genes (Kreps et al., 2002; Wang et al., 2014). HSFs are

* Corresponding author.
E-mail address: pshashi@bhu.ac.in (S.P. Rai).

https://doi.org/10.1016/j.jbiotec.2020.01.001
Received 11 November 2019; Received in revised form 17 December 2019; Accepted 3 January 2020
Available online 11 January 2020

activated after binding to heat shock elements (HSEs; 5′-AGAAnnTTCT-3′) (Vihervaara., 2013). Plant HSF proteins have highly conserved N-terminal DNA binding domain (DBD) characterized by the presence of pivotal helix-turn-helix motif that binds to HSE and initiates transcription of stress-inducible genes (Scharf et al., 2012; Guo et al., 2016). C-terminal domains of plant HSFs are distinguished by the presence of both activation domain containing AHA motifs formed by large acidic, aromatic and hydrophobic amino acid residues and repressor domain (RD) characterized by the presence of tetrapeptide LFGV (Ikeda and Ohme-Takagi, 2009; Fragkostefanakis et al., 2015).

In our previous work (Rai et al., 2018b), we studied individual effect of different concentrations of SA and SNP on HT stressed *Lablab purpureus* L. This study is a step forward form our previous work, where we investigated whether interaction between SA and SNP can improve growth, reproduction, physiology of HT stressed *Lablab purpureus* L. We then examine whether their interactive effect can cause induction of genes involved in secondary metabolic pathway or whether their individual applications are more effective. Extensive literature survey has revealed that till date no information is available regarding the expression of the heat shock transcription factors (HSFs) in L. *purpureus* as it is still considered as “Orphan Crop” for its genome revolution (Rai et al., 2018d). Therefore, *in-silico* approaches were also adopted to provide a comprehensive analysis of evolutionary aspects and putative functions of HSF in response to HT stress and their functional divergence and evolution in other legume crops.

2. Materials and methods

2.1. In-vitro studies

2.1.1. Plant growth and treatments

Hyacinth bean (*Lablab purpureus* L. cv. VRBSEM-15) seeds of uniform size were selected, sterilized with sodium hypochlorite solution (NaOCl, 2 %) and washed rigorously by distilled water. The seeds were then subjected to HT stress by sowing them in the field at the research farm of Indian Institute of Vegetable Research, Varanasi (U.P) in the month of April-June 2017. The soil of the field was sandy loam soil containing farmyard manure in 3:1 ratio with plot dimension of 2 m × 5 m. The mean environmental conditions during the entire experimental work were: maximum/minimum temperatures 36.6 ± 5.1 °C/ 30.3 ± 6.6 °C, 12 h of light/ dark photoperiod, and mean relative humidity (RH) of 75.6 ± 5.5. The plants were irrigated twice a week during the entire course of investigation (Supporting Information Table S4). Exogenous individual supplementation (foliar spray) of salicylic acid (SA 0.5 and 1.0 mM), sodium nitroprusside SNP (0.5 mM) and their combination *viz.,* SA + SNP (0.5 + 0.5 mM) and SA + SNP (1.0 + 0.5 mM) was done after the plants have attained their vegetative state (21 days after sowing). Both the compounds used for exogenous applications were of technical grade (HiMedia Laboratories, India). Each treatment (five treatments along with non-treated control) had three plots as triplicates and each plot had 20 plants. Since the entire experiment was conducted in high-temperature environment (April to June) in open field condition, the inclusion of control plants grown in normal condition was not possible. So, we have used non-treated high temperature stressed plants as control. All the plants of VRBSEM-15 were of determinate (Bush type) growth habit and were not trimmed during the entire experimental period. The foliar spray of SA, SNP and their combinations were arranged in four applications i.e. first treatment was done on 21st day of germination (DOG), and second third and fourth on 28th, 35th and 42nd DOG by compression sprayer in the evening (capacity 2.5 L, nozzle diameter of 34 mm and mixed with tween-20) till the respective doses of each phytohormone were achieved. Finally, the experiment was terminated by allowing plants to grow in the same condition for seven more days without any application and the samples (fully expanded leaf, third from bottom) were collected on the 50th day and stored at −80 °C for various analysis.

2.1.2. Measurement of physiological parameters and yield

Photosynthetic photon flux density (PPFD) in treated and non-treated plants were measured in terms of μm s^{-1} m^{-2} by Licor-Li189 (USA) from the fully expanded leaf (third from top). Infrared thermometer (Spectrum Technologies Inc. China) was used to measure leaf canopy temperature a distance of 30 cm from the surface of the leaf. Chlorophyll content (CCI) index was measured by the Chlorophyll Content Meter (CCM 200, Apogee Instruments Inc. USA) from the fully expanded leaf (third from top) and mean of three readings was used for each treatment. Fluorescence variable and fluorescence maximum (Fv/Fm) was also measured on 30-min dark-adapted fully expanded leaves by Hansatech Handypea (USA) meter. Leaf water content in leaf discs of uniform size was estimated by measuring fresh weight (FW), dry weight (DW) and turgid weight (TW) as per the method given by Turner and Kramer (1980). Electrolytic leakage (Deshmukh et al., 1991) was estimated by measuring the conductivities (C) of leaf discs (C1 at 40 °C and C2 at 100 °C) by the conductivity meter (Century Instruments, Chandigarh, India). The number of pods and yield per plant were measured form randomly chosen 10 plants from each treatment.

2.1.3. Measurement of chlorophyll and carotenoid content

The photosynthetic pigment contents were measured by extracting leaf samples (300 mg) in 80 % acetone as described by Porra et al. (1989). The absorbance of the supernatant was recorded at 480, 510, 645 and 663 nm by a UV–vis spectrophotometer (Perkin Elmer, Elico Ltd. China). The amount of photosynthetic pigments was measured as per the equation given by Arnon (1949) and expressed as mg g^{-1}FW.

2.1.4. Estimation of lipid peroxidation and proline level

Lipid peroxidation was measured (Heath and Packer, 1968) by extracting 200 mg of leaf samples in 5 ml of tri-chloroacetic acid (10 % TCA) and 2-thiobarbituric acid (0.25 % of TBA) mixture. The absorbance was recorded at 532 and 600 nm and membrane damage were calculated using extinction coefficient of 155 mM^{-1} cm^{-1} and expressed as μmol g^{-1} FW. Estimation of proline was done as per the standard protocol devised by Bates et al. (1973). Leaf samples were extracted in the mixture of sulfosalicylic acid, glacial acetic acid, and ninhydrin. The mixture was centrifuged at 8000 rpm. The resulting supernatant was then mixed with toluene (4 ml) and incubated at 100 °C for 1 h. The absorbance of chromophore was recorded at 520 nm and expressed as μg g^{-1} FW.

2.1.5. Measurement of free oxygen radicals

Hydrogen peroxide content (H_2O_2) was measured by extracting sample in sodium phosphate buffer (Jana and Choudhuri, 1981). The absorbance of yellow colour supernatant containing 0.1 % titanium sulphate was recorded at 410 nm. The generation of H_2O_2 was measured using an extinction coefficient of 0.28 μM^{-1} cm^{-1} and expressed as μmol g^{-1} FW. Superoxide $(O_2)^{\cdot}$ anion radicals' generation was estimated as described by Misra and Fridovich (1972). Leaf samples were homogenized in potassium phosphate buffer containing sucrose, $MgCl_2$, and diethyl di-thiocarbamate. The mixture was centrifuged at 12,000 rpm for 20 min and absorbance of the supernatant was measured at 540 nm. The extent of superoxide anion generation was calculated (using an extinction coefficient of 4 mM^{-1} cm^{-1}) and expressed as Δ_{A540} min^{-1} mg^{-1}protein.

2.1.6. Measurement of enzymatic and non-enzymatic antioxidants

The activity of catalase (CAT; EC: 1.11.1.6) was estimated as per the protocol devised by McKersie et al. (1990). Leaf samples (200 mg) were extracted in Tris NaOH buffer (50 mM, pH 8.0). The absorbance of the assay mixture containing enzyme extract, substrate and buffer were measured at 240 nm (for 5 min). The specific activity was calculated using an extinction coefficient of 0.036 mM^{-1} cm^{-1} and expressed as μmol of H_2O_2 oxidized min^{-1} mg^{-1} protein.

The assay for ascorbate peroxidase (APX; EC: 1.11.1.11) activity

was done by following the protocol described by Nakano and Asada (1981). About 200 mg of leaf tissue was homogenized in potassium phosphate buffer (50 mM, pH 7.8). The absorbance of ascorbate oxidation in the reaction mixture was noted at 290 nm. Specific activity was calculated by using an extinction coefficient of 2.8 mM^{-1} cm^{-1} and expressed as µmol ascorbate oxidized min^{-1} mg^{-1} protein.

Glutathione reductase (GR; EC: 1.6.4.2) activity was estimated by extracting leaf tissue (200 mg) Tris − HCl buffer (100 mM, pH 7.8). The absorbance of the reaction mixture was recorded at 340 nm (Rodriguez Sanchez et al., 2010). Specific activity of the enzyme was calculated by using extinction coefficient 6.2 mM^{-1} cm^{-1} and expressed as µmol NADPH oxidized min^{-1} mg^{-1} protein.

The activity of superoxide dismutase (SOD; EC: 1.15.1.1) was determined by the method described earlier (Shah et al., 2001). Approx. 200 mg of leaf samples were extracted in the potassium-phosphate buffer (pH 7.5). The absorbance of supernatant containing enzyme extract, EDTA and epinephrine was noted at 470 nm and expressed as unit min^{-1} mg^{-1} protein.

Monodehydroascorbate reductase (MDHAR; EC: 1.6.5.4) activity was measured by extracting the leaf samples (200 mg) HEPES − HCL (100 mM) as described by Rodriguez-Sanchez et al. (2010). The absorbance of the reaction mixture was recorded at 340 nm. Specific activity was calculated using an extinction coefficient of 6.2 mM^{-1} cm^{-1} and expressed as µmol ascorbate oxidized min^{-1} mg^{-1} protein.

Dehydroascorbate reductase (DHAR; EC: 1.8.5.1) activity was assayed as per the published method (Nakano and Asada, 1981) by extracting the leaf samples (200 mg) in sodium phosphate buffer (25 mM, pH 7.0). The absorbance of the supernatant was noted at 265 nm. Specific activity was calculated using an extinction coefficient of 14 mM^{-1} cm^{-1} and expressed as µmol NADPH oxidized min^{-1} mg^{-1} protein.

Ascorbate (AsA) assay was measured by extracting leaf samples in the mixture of meta-phosphoric acid and EDTA (Law et al., 1983). The reaction mixture containing supernatant, sodium phosphate buffer (150 mM), dithiothreitol (DTT), N-ethylmaleimide (0.5 % w/v), 2,2′-bipyridyl (4 % w/v), ortho-phosphoric acid (44 % v/v) and $FeCl_3$ (3 % w/v) was incubated for 30 min in dark. The absorbance was recorded at 525 nm and the content was calculated by using calibration plot of standard AsA.

Glutathione (GSH) content was estimated by extracting leaf sample in 100 mM potassium phosphate buffer as described previously (Owens and Belcher, 1965). The absorbance of supernatant containing NADPH (0.25 mM) and glutathione reductase (0.5 units) was measured at 412 nm and standard calibration plot of GSH (1 − 10 µg) was used to calculate the final concentration.

2.1.7. Measurement of pollen viability and in-vitro pollen germination

Viability of pollen grains was measured by acetocarmine calorimetric staining method (Wang et al., 2004a). Pollen viability was assessed under fluorescence microscope (Leica DMi8), pollen grains with dark red colour were considered as viable whereas colourless pollens were classified as non-viable. For estimation of *in-vitro* pollen germination and tube growth, pollens collected from five different flowers were cultured in pollen culture medium comprising of 10 % sucrose, 100 µg g^{-1} H_3BO_3, 250 µg g^{-1} Ca $(NO_3)_2$• $4H_2O$, 200 µg g^{-1} $MgSO_4$•$7H_2O$ and 100 µg g^{-1} KNO_3 for 4 h at 25 °C (Brewbaker and Kwack, 1963). Pollen was considered as germinated when pollen tube length surpassed the width of the pollen grain. The percentage of viable and non-viable pollen, as well as germination, was measured by observing 100 pollen grains.

2.1.8. Histochemical detection of H_2O_2 and $O_2^{\bullet-}$

Diaminobenzidine (DAB) and nitro-blue tetrazolium chloride (NBT) staining method were used to detect the possible generation of H_2O_2 and $O_2^{\bullet-}$ in the leaves. The leave samples were first incubated in DAB (1 mg/ml, pH 3.8) and NBT (0.1 mg/ml) solutions for 24 h at 25 °C (Jabs et al., 1996; Thordal-Christensen et al., 1997). After the appearance of blue (NBT staining) and brown spots (DAB staining), samples were destained using 70 % ethanol to remove chlorophyll and picture was captured using digital camera. The relative intensity of DAB and NBT was measured by using ImageJ software (National Institutes of Health, Bethesda, MD, USA).

2.1.9. HT-induced anatomical changes

Cross-sections of stem treated with SA, SNP and their combinations were prepared from freshly harvested parts with razor blades and stained with 0.25 % safranin (prepared in 50 % ethanol), mounted on a glass slide with dibutyl phthalate xylene (DPX). The samples were then subjected to gradual dehydration with 20–100 % ethanol for 5 min and observed under Dewinter image microscope (Dewinter Technologies, Italy). The images obtained were subjected to further analysis using ImageJ software.

2.1.10. Protein estimation

The estimation of soluble protein in each sample was done as per the method described previously (Lowry et al., 1951) using BSA as a standard.

2.1.11. RNA isolation and cDNA preparation and Real-time Quantitative PCR analysis

TRIZOL reagent (Invitrogen) was used to isolate total RNA following the manufacturer's recommendations. The purity of isolated RNA was assessed by recording its absorbance ratio at 230/260/280 nm and the quality was assessed on agarose gel electrophoresis (1.0 %). The cDNA strands (1.0 µg of total RNA) were synthesised by using iscript™ cDNA synthesis kit (Bio-Rad Laboratories, USA) following manufacturer's instructions. Further, real-time Quantitative PCR reactions (qRT PCR) were executed by SsoFast™ EvaGreen® Supermix detection chemistry (Bio-Rad) in iQ5 thermocycler (BioRad Laboratories, USA). The accessed sequence from GenBank was used to design stress-responsive primers (Supporting information, Table S1) using Primer 3 software (version 0.4.0, http://www.bioinfo.ut.ee). The qRT amplification programs (in three biological and technical replicates) were: initial denaturation at 95 °C for 10 min, 45 cycles of denaturation at 95 °C for 15 s, annealing at 60 °C for the 30 s and final extension at 72 °C for 30 s. The relative amplification profiles of all the stress-responsive genes were evaluated by normalizing to the C_t data of the *ACTIN* gene (5′-GTGTC TGGATTGGAGGATCAATC-3′,5′-GGCCACGCTCATCATATTCA-3′) as an internal control using $2^{-\Delta\Delta CT}$ method (Livak and Schmittgen, 2001). The resulting data was then analysed by using Bio-conductor R (http://www.bio conductor.org) to generate heat-map whereas the specificity of the amplified products was assessed by performing melt curve analysis and recording the fluorescence at 520 nm.

2.2. In-silico studies

2.2.1. Database search and comparative phylogeny

Hyacinth bean (*Lablab purpureus* L.) is considered as an "Orphan crop" in context to its genome revolution. Due to unavailability of genome sequencing data for this crop, we have retrieved the coding sequences for heat shock transcription factor (HSF) from drought inducible ESTs data specific to L. *purpureus* for sequence alignment and phylogenetic studies. Since the EST sequence retrieved encoded the partial HSF protein, we have searched the protein sequence of HSF from other model legume crop (*Glycine max*) having close ancestry to L. *purpureus* to provide a comprehensive analysis of evolutionary lineages observed in the legume evolution. The plant transcription factor database (PlantTFDB) http://planttfdb.cbi.pku.edu.cn/ (Jin et al., 2014) was used for retrieving the complete list of all the putative HSF TFs available and sequence of the first hit (Glyma.01G015900.1.p) was used for further studies.

2.2.2. Sequence alignment and phylogenetic analysis

The full-length protein was further annotated and checked using BLASTx tool. The coding sequences of the protein was obtained using tBLASTn programme, and were searched against the Expressed sequence tag (ESTs) database for L. *purpureus* (taxid: 35,936). The first significant hit obtained was subjected to BLASTp annotation for finding the sequential homologs and orthologs to *L. purpureus*. The sequences were further aligned using the Clustal W program and edited using BioEdit tool. Multiple sequence alignment for all the retrieved homologs and orthologues were performed using CLC Bio work-bench. The phylogenetic tree was constructed by MEGA 6.0 suite http://www.megasoftware.net/ (Tamura et al., 2013) using Unweighted Pair Group Method with Arithmetic Mean (UPGMA) and maximum parsimony (MP) method with 1000 replication bootstrap values. The sequential similarities and differences found in HSF02 proteins between different homologous and orthologous were visualized using Circos visualization tool http://circos.ca/ (Krzywinski et al., 2009) at maximum 75 % cut-off filter values. Further, the functional domain within the protein sequences was identified using ExPASy-Prosite scan http://prosite.expasy.org/scanprosite/ (De Castro et al., 2006).

2.2.3. Gene prediction and promoter analysis

The protein sequence of HSF02 (*Glycine max*) were analysed using tBLASTn programme and searched across the whole genome contig database (wgs). The position of CDS encoding for HSF02 was searched in the nucleotide sequences of the genomic DNA. The sequences present in reverse orientation/negative frame were converted to the positive frame using the reverse complement (link) tool. The position of CDS including the transcriptional start sites (TSS), and polyadenylation signal (polyA) tail was retrieved using Fgenesh server http://www.softberry.com (Salamov and Solovyev., 2000) Further, the structural organization of HSF02 gene was explored using the nucleotide sequences given for CDS and complete gene (including promoter) using Gene display server (GSDS 2.0) http://gsds.cbi.pku.edu.cn/ (Hu et al., 2014).

2.2.4. Structural modelling and model validation

The available protein sequence for the HSF02 was searched across the Protein Data Bank (rcsb.org/pdb/) for finding the closely related structural homologue for the queried sequence using BLASTp program for homology modelling (Berman et al., 2000). Identification of putative templates in HSF02 protein sequences was done using NCBI BLASTp program. The three most closely related templates exhibiting significant similarity with our queried sequence and whose sequenced are resolved by X-ray diffraction were used for structural modelling of the functional domain using SWISS-MODEL server http://swissmodel.expasy.org/ (Biasini et al., 2014). Three models were generated by swiss modeller based on the available crystal structures of human Hsf1 with HSE DNA (PDB ID: 5D5U), the crystal structure of heat shock factor1-DBD complex (PDB ID: 5HDN) and crystal structure of heat shock factor 1-DBD (PDB ID: 5HDG). The models were further refined by two-step atomic-level energy minimization based on Cα traces using ModRefiner http://zhanglab.ccmb.med.umich.edu/ModRefiner/ (Xu and Zhang, 2011). The modelled protein was further validated based on their qualitative and quantitative score values. The model having the least energy values were further selected as the final model for further studies. The qualitative assessments were done using ProSA https://prosa.services.came.sbg.ac.at/ (Wiederstein and Sippl, 2007), Qmean https://swissmodel.expasy.org/qmean/ (Benkert et al., 2009), RESPROX (Resolution by Proxy), ERRAT http://services.mbi.ucla.edu/ERRAT/stats/ (Colovos and Yeates, 1993) and the quantitative assessment was carried out using VADAR (Volume, Area, Dihedral Angle Reporter) http://vadar.wishartlab.com/ analysis (Willard et al., 2003). Ramachandran plot was used for the validation of the stability of the predicted HSF02 model by measuring the backbone dihedral phi (φ) and psi (Ψ) angles using PROCHECK module of PDBSum server http://www.ebi.ac.uk/pdbsum/ (Laskowski et al., 2005) and further confirmed by RAMPAGE server http://mordred.bioc.cam.ac.ik/~rapper/rampage.php (Lovell et al., 2003). The protein models generated for the functional domain were further submitted to an online repository PMDB (Castrignano et al., 2006) to obtain the accession identities.

2.2.5. DNA-protein interaction

The DNA protein interaction was done using Hex docking server (Macindoe et al., 2010) and following parameters were used for docking calculations i.e. Shape + Electro + DARS, FFT Mode-3D fast lite and grid range of 0.6 with Receptor: Ligand: Twist: Distance range of 180: 180: 360: 40. Discovery Studio 3.0 was used to visualize the interaction between docked complexes. The DNA-protein complex having the least binding energy values were further selected for analysing the key residues involved in binding with DNA.

2.2.6. Protein-protein interaction, structural and functional annotation

The STRING (Search Tool for the Retrieval of Interacting Genes/Proteins) database version 10.0 http://string-db.org/ was used to predict protein interaction partners for HSF02 (Szklarczyk et al., 2015). The interaction results were obtained at the high confidence values using several parameters such as co-expression, co-occurrence, neighbour, gene fusion, text-mining and experiments at confidence score of 0.40 with interaction from both shells of interactors. Structural classification of HSF02 protein was done by using CATH server http://www.cathdb.info/ (Sillitoe et al., 2015) and functional classification of the identified CATH super-families was done by using FunFHMMer http://www.cathdb.info/search/by-funfhmmer (Das et al., 2016). The functional annotation of HSF02 protein was further analysed for its gene ontology study by using hypergeometric distribution test analysis of REVIGO web-server http://revigo.irb.hr/ (Supek et al., 2011) and the identified GO values were further subjected to CELLO2GO web-server http://cello.life.nctu.edu.tw/cello2go/ (Yu et al., 2014) to find out its probable subcellular localization.

2.3. Statistical analysis

All the experiments were performed in three biological replications and subjected to analysis of variance (ANOVA). The mean differences were compared by performing Duncan's multiple range test (DMRT) using SPSS software (SPSS Inc., Version 20.0) and values at $P \leq 0.05$ were considered significant.

3. Results

3.1. Plant physiology and yield

The application of exogenous SA (1.0 mM), SA + SNP (0.5 + 0.5 mM) and SA + SNP (1.0 + 0.5 mM) alleviated the effect of HT stress more prominently compared to other treatments by enhancing photosynthetic efficiency (41.0–49.0 %) and chlorophyll colour index (29.0–38.7 %) compared to non-treated HT stressed control plants (Table 1). Further, yield and related attributes decreased significantly under HT stress. However, significant increase in the number pods (110.1–205.5 %) and yield/plant (103–205.5 %) was noticed upon foliar application of SA (1.0 mM), SA + SNP (0.5 + 0.5 mM) and SA + SNP (1.0 + 0.5 mM) compared to non-treated HT stressed control.

3.2. Plant water status and photosynthetic pigments content

Relative water content, chlorophyll, and carotenoid contents decreased significantly in HT stressed VRBSEM-15 plants (Table 2). However, the application of SA, SNP and their combinations assuaged the adverse effect of HT on these attributes. Exogenous application of SA (1.0 mM), SA + SNP (0.5 + 0.5 mM) and SA + SNP (1.0 + 0.5 mM) mitigated the injurious effect of HT and significantly improved

Table 1
Effects of different levels of salicylic acid (SA) and sodium nitroprusside (SNP) and their combinations on photosynthetic photon flux density (PPFD), chlorophyll colour index (CCI), Fv/Fm, number of pods per plant (NPP) and yield per plant (YPP) in *Lablab purpureus* L. (cv VRBSEM-15) plants under high temperature stress.

Treatments	PPFD ($\mu m\ s^{-1}\ m^{-2}$)	Canopy temperature (°C)	CCI (%)	Fv/Fm	NPP	YPP (g/plant)
NT	1122.13 + 1.47^{ab}	33.4 + 0.61^{a}	31.5 + 0.78^{c}	0.53 + 0.14^{c}	36.0 + 1.77^{d}	180 + 0.15^{d}
SA (0.5 mM)	1207.43 + 2.82^{a}	31.7 + 0.38^{a}	34.6 + 1.04^{a}	0.64 + 0.06^{ab}	57.3 + 1.71^{c}	286 + 0.11^{b}
SA (1.0 mM)	1013.90 + 4.34^{b}	32.8 + 0.73^{a}	43.3 + 0.71^{bc}	0.75 + 0.09^{a}	73.3 + 1.11^{c}	366 + 0.16^{c}
SNP (0.5 mM)	1159.90 + 5.14^{ab}	30.9 + 0.49^{a}	38.0 + 1.29^{abc}	0.64 + 0.10^{bc}	65.6 + 1.06^{c}	328 + 0.18^{b}
SA + SNP (0.5 + 0.5 mM)	1066.53 + 3.71^{ab}	30.8 + 0.55^{a}	40.0 + 0.37^{ab}	0.74 + 0.06^{a}	86.0 + 1.11^{a}	430 + 0.24^{a}
SA + SNP (1.0 + 0.5 mM)	1078.33 + 4.55^{ab}	31.9 + 0.32^{a}	43.5 + 0.93^{a}	0.79 + 0.09^{bc}	110.6 + 1.54^{b}	550 + 0.16^{bc}

Mean (+ SE) was calculated from three replicates for each treatment. Values with different letters are significantly different at $P \leq 0.05$ applying the LSD test, NT: non-treated HT stressed control.

relative water content (17.3–27.8 %), chlorophyll (67.2–103.9 %) and carotenoid (27.5–38.0 %) content more influentially than SA (0.5 mM), SNP (0.5 mM) compared to non-treated HS control (Table 2).

3.3. Membrane damage, ROS generation, and proline

The level of lipid peroxidation, electrolytic leakage, hydrogen peroxide, and superoxide anion radical increased by 44.8 %, 45.0 %, 72.0 % and 89 % in non-treated control VRBSEM-15. Exogenously applied SA (1.0 mM), SA + SNP (0.5 + 0.5 mM) and SA + SNP (1.0 + 0.5 mM) significantly reduced lipid peroxidation (45.9–55.0 %), electrolytic leakage (37.0–45.0 %) and ROS level (42.2–89.0 %) more competently than SA (0.5), SNP (0.5) under HT stress (Table 3). Furthermore, the level of osmolyte proline was also significantly affected upon the application of SA, SNP and their combination under HT stress. Higher level of proline (50.0–121.6 %) was observed in SA (1.0 mM), SA + SNP (0.5 + 0.5 mM) and SA + SNP (1.0 + 0.5 mM) treated VRBSEM-15 plants compared to non-treated HT stress control (Table 3).

3.4. Activities of enzymatic and non-enzymatic antioxidants

The specific activity of CAT exhibited significant increase (60–140 %) in SA (0.5 mM), SA (1.0 mM) and SA + SNP (1.0 + 0.5 mM) treated VRBSEM-15 plants compared to non-treated HT stress control (Fig. 1a). Ascorbate peroxidase activity showed approximately 80–140 % increase in SA (1.0 mM), SA + SNP (0.5 + 0.5 mM) and SA + SNP (1.0 + 0.5 mM) treatments compared to their corresponding counterparts (Fig. 1b). Glutathione reductase activity was stimulated upon application of SA (1.0 mM) and SA + SNP (1.0 + 0.5 mM) (Fig. 1c). The GR activity also significantly increased in SA (0.5 mM), SNP (0.5 mM) and SA + SNP (0.5 + 0.5 mM) but the magnitude was comparatively low (Fig. 1c). Superoxide dismutase activity decreased significantly under HT stress. However, application of SA (1.0 mM) SA + SNP (0.5 + 0.5 mM) and SA + SNP (1.0 + 0.5 mM) increased the SOD activity by 200–253 % more competently than SA (0.5 mM), SNP (0.5 mM) and non-treated plants (Fig. 1d).

A sharp decrease in the DHAR activity was detected under HT stress. Compared to treated plants, DHAR activity decreased by 30.4–195.1 % in non-treated control plants (Fig. 2a). However, applications of SA (1.0 mM) SA + SNP (0.5 + 0.5 mM) and SA + SNP (1.0 + 0.5 mM) amplified the DHAR activity by 117.3–195.1 % compared to non-treated control plants (Fig. 2a). SA, SNP and their combination increases MDHAR activity by 400–600 % in HT stressed VRBSEM-15 plants, where maximum increased was observed in plants treated with SA (1.0 mM) SA + SNP (0.5 + 0.5 mM) and SA + SNP (1.0 + 0.5 mM) respectively (Fig. 2b). Foliar application of SA (0.5 mM) and SA + SNP (0.5 + 0.5 mM) significantly improved the AsA content by 100–150 % compared to the control plants (Fig. 2c). The AsA content also increases in other treatments but the increased was of lower magnitude compared to SA (0.5 mM) and SA + SNP (0.5 + 0.5 mM) treatments. Levels of glutathione in exogenous applied SA, SNP and their combination increased by 50–80 % compared to non-treated control (Fig. 2d). The levels remain approximately the same in all the treatments, however, the maximum increase in glutathione level was observed for SA (1.0 mM) and SA + SNP (1.0 + 0.5 mM) treatments.

3.5. Pollen viability and in-vitro pollen germination

Pollen viability decreased up to 64.2 % in non-treated control plants and from 7.1 to 34.4% in SA and SNP treated plants (Fig. 3a). However, foliar application of SA, SNP and their combination mitigated the adverse effect of HT stress and improve the viability of the pollen grains by 61.3–92.5 %. Maximum viability was observed SA (0.5 and 1.0 mM) SA + SNP (0.5 + 0.5 mM) and SA + SNP (1.0 + 0.5 mM) treated plants (Figs. 3a and S2a). HT stress also adversely affected pollen germination rate and pollen tube growth in differentially treated and non-treated VRBSEM-15 plants (Fig. 3a and b). However, the application of SA and SNP significantly improved the pollen germination rate. Highest germination percentage was observed in SA (0.5 and 1.0 mM) and SA + SNP (1.0 + 0.5 mM) treated plants (Fig. 3a). Results of Pollen tube growth was grouped into three categories *viz.*, no tube, half tube and full tube growth (Figs. 3b and S2b). The maximum percentage of full pollen tube growth was recorded for SA (0.5 and 1.0 mM) and SA + SNP (1.0 + 0.5 mM) treatments compared to non-treated plants under HT stress.

Table 2
Effects of different levels of salicylic acid (SA) and sodium nitroprusside (SNP) and their combinations on chlorophyll *a* (Chl a), chlorophyll b (Chl b), total chlorophyll (T Chl) carotenoid (Car) and relative water content (RWC) in *Lablab purpureus* L. (cv VRBSEM-15) plants under high temperature stress.

Treatments	Chl a (mg g^{-1}FW)	Chl b (mg g^{-1}FW)	T Chl (mg g^{-1}FW)	Car (mg g^{-1}FW)	RWC (%)
NT	1.87 + 0.09^{e}	0.89 + 0.04^{d}	2.78 + 0.15^{d}	1.38 + 0.12^{b}	46.0 + 0.12^{c}
SA (0.5 mM)	2.28 + 0.12^{c}	1.76 + 0.13^{c}	4.14 + 0.14^{c}	1.55 + 0.12^{a}	50.7 + 0.12^{b}
SA (1.0 mM)	2.52 + 0.10^{b}	2.23 + 0.12^{b}	4.85 + 0.14^{b}	1.76 + 0.16^{a}	56.3 + 0.16^{a}
SNP (0.5 mM)	2.01 + 0.15^{d}	0.91 + 0.05^{d}	2.94 + 0.19^{d}	1.39 + 0.13^{b}	47.5 + 0.13^{bc}
SA + SNP (0.5 + 0.5 mM)	2.90 + 0.13^{a}	2.73 + 0.13^{a}	5.67 + 0.16^{a}	1.78 + 0.17^{a}	54.0 + 0.17^{ab}
SA + SNP (1.0 + 0.5 mM)	2.55 + 0.14^{b}	2.16 + 0.11^{b}	4.65 + 0.17^{b}	1.85 + 0.12^{a}	58.8 + 0.12^{abc}

Mean (+ SE) was calculated from three replicates for each treatment. Values with different letters are significantly different at $P \leq 0.05$ applying the LSD test, NT: non-treated HT stressed control.

Table 3
Effects of different levels of salicylic acid (SA) and sodium nitroprusside (SNP) and their combinations on hydrogen peroxide (H_2O_2), superoxide anion ($O_2^{\bullet -}$), proline (PRO), lipid peroxidation (LPO) and electrolytic leakage (EL) in *Lablab purpureus* L. (cv VRBSEM-15) plants under high temperature stress.

Treatments	H_2O_2 (μm g^{-1}FW)	$O_2^{\bullet -}$ (ΔA540 min^{-1} mg^{-1} protein)	PRO (μg g^{-1}FW)	LPO (mm g^{-1}FW)	EL (%)
NT	40.5 + 0.48^{a}	1.00 + 0.07^{a}	39.8 + 0.57^{e}	2.70 + 0.14^{a}	35.1 + 0.14^{a}
SA (0.5 mM)	25.4 + 0.37^{f}	0.45 + 0.03^{e}	52.7 + 0.54^{a}	1.67 + 0.15^{d}	24.5 + 0.15^{b}
SA (1.0 mM)	11.3 + 0.38^{c}	0.15 + 0.05^{c}	60.0 + 0.59^{c}	1.46 + 0.13^{d}	19.3 + 0.13^{a}
SNP (0.5 mM)	23.4 + 0.44^{b}	0.23 + 0.04^{d}	53.9 + 0.89^{d}	2.06 + 0.12^{b}	29.2 + 0.12^{ab}
SA + SNP (0.5 + 0.5 mM)	15.7 + 0.45^{e}	0.11 + 0.05^{f}	71.1 + 0.44^{b}	1.27 + 0.14^{d}	22.1 + 0.14^{ab}
SA + SNP (1.0 + 0.5 mM)	18.0 + 0.39^{d}	0.19 + 0.06^{b}	88.2 + 0.83^{d}	1.18 + 0.12^{c}	20.8 + 0.12^{ab}

Mean (+ SE) was calculated from three replicates for each treatment. Values with different letters are significantly different at $P \leq 0.05$ applying the LSD test, NT: non-treated HT stressed control.

3.6. Histochemical detection of H_2O_2 and $O_2^{\bullet -}$

The sites for biological accumulation of H_2O_2 and $O_2^{\bullet -}$ was analysed by staining them with DAB and NBT (Fig. 4a and b). The H_2O_2 accumulation sites were characterized with intense dark brown coloration whereas sites for $O_2^{\bullet -}$ were characterized by dark blue spots. Higher accumulation of both H_2O_2 and $O_2^{\bullet -}$ was observed at the leaf margin and tip as these regions showed intense colouration under microscopic view. However, foliar application of SA, SNP and their combinations significantly ameliorated the toxic effect of HT stress and decreases the rate of H_2O_2 and $O_2^{\bullet -}$ generation by 50 % and 66.6 % compared to non-treated control (Supporting information, Fig. S3a and b).

3.7. Anatomical changes in stem

HT stress significantly increased the cortex diameter by 40 % and decreased the diameter of xylem (12.2 %) and phloem cells (16.6 %) in non-treated control plants (Supporting information, Fig. S4). Likewise, the number and diameter of vessels were also decreased in non-treated plants under HT stress (Fig. 4c). However, foliar applications of SA, SNP, and their combinations significantly improved the number and diameter of xylem, phloem, vessels and limits the diameter of cortex by 11.3, 15.3, 44.4 % respectively as compared to non-treated controls.

3.8. Expression analysis of stress-responsive genes

Effect of SA, SNP and their combinations on the expression of stress-responsive genes such as ATP synthase CF1 alpha subunit (*ATP synthase*), chlorophyll *a*/b binding protein (*Chl a/b*), lipid transfer protein (*LTP*), Heat shock factor (*HSF*), zinc finger protein (*ZFP*), thioredoxin h (*TRX*), late embryogenesis abundant protein (*LEA*), dicarboxylate transporter (*DCT*) and elongation factor 1 alpha (*EF1α*) under HT stress in VRBSEM-15 plants has been shown in Fig. 5. Treating plants with SA (0.5 and 1.0 mM), SA + SNP (0.5 + 0.5 mM) and SA + SNP (1.0 + 0.5 mM) induced the expression of HSF by 7.0–18.0 % and thioredoxin h by 7.1–15.0 % (Fig. 5). Further, results also showed the upregulation of *LEA, EF1α, Chl a/b,* and *ATP synthase* genes in all the treatments compared to non-treated control where the upregulation of these genes was also more pronounced in SA (0.5 and 1.0 mM), SA + SNP (0.5 + 0.5 mM) and SA + SNP (1.0 + 0.5 mM) treated plants. We also noted that

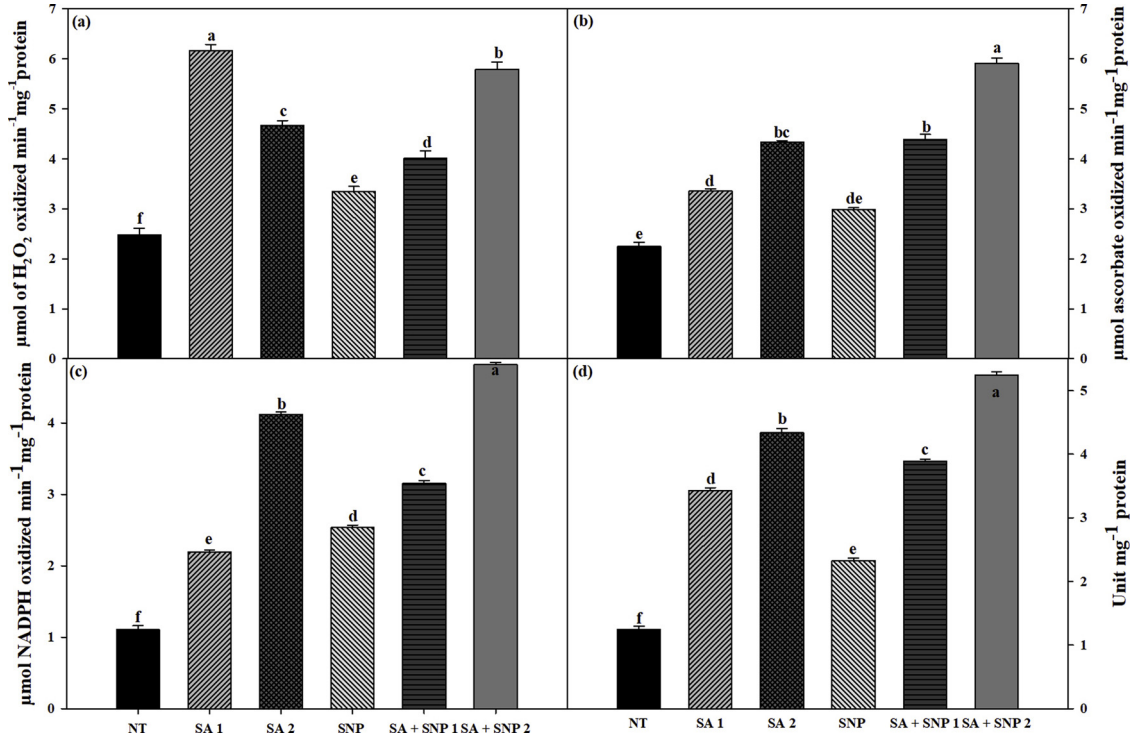

Fig. 1. Aftereffect of different levels of salicylic acid (SA) and sodium nitroprusside (SNP) and their combinations on (a) catalase (CAT), (b) ascorbate peroxidase (APX), (c) glutathione reductase (GR) and (d) superoxide dismutase (SOD) activities in *Lablab purpureus* L (cv VRBSEM-15) under high temperature stress. Mean (± SE) was calculated from three replicates for each treatment. Bars with distinct letters are significantly different at $P \leq 0.05$ applying the DMRT test. NT: non-treated HT stressed control, SA 1 (0.5 mM), SA 2 (1.0 mM), SNP (0.5 mM), SA + SNP 1 (0.5 + 0.5 mM) and SA + SNP 2 (1.0 + 0.5 mM).

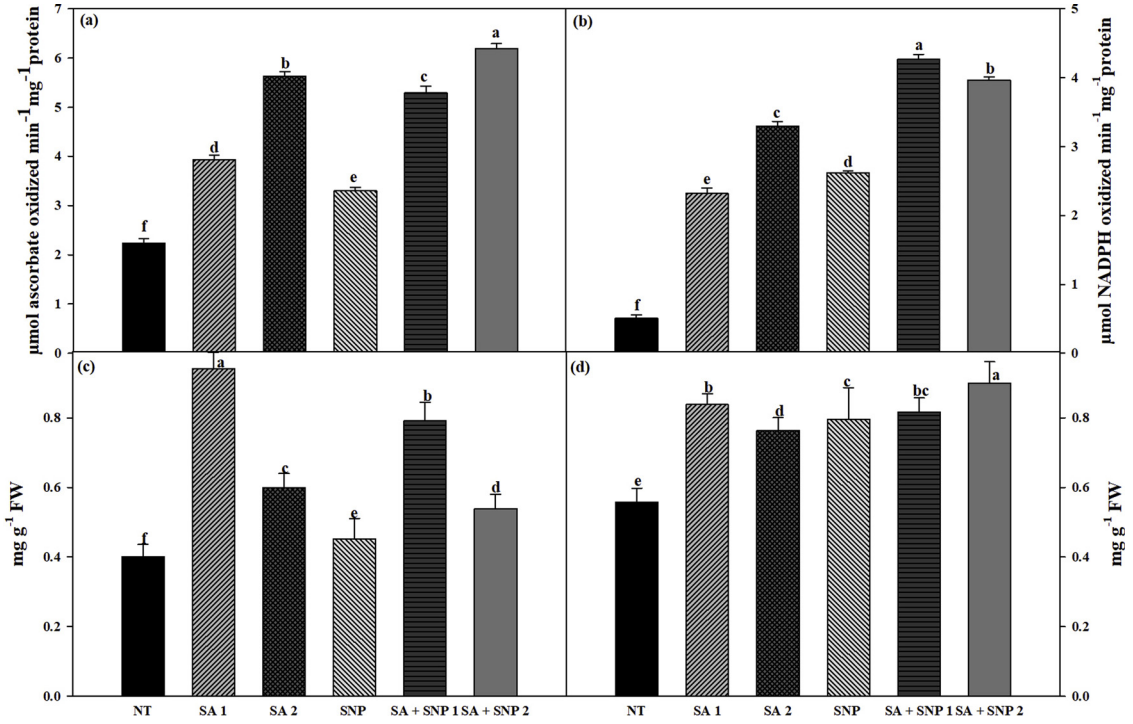

Fig. 2. Aftereffect of different levels of salicylic acid (SA) and sodium nitroprusside (SNP) and their combinations on (a) dehydroascorbate peroxidase (DHAR), (b) mono-dehydroascorbate reductase (MDHAR), (c) ascorbate (AsA) and (d) glutathione (GSH) activities in *Lablab purpureus* L (cv VRBSEM-15) under high temperature stress. Mean (± SE) was calculated from three replicates for each treatment. Bars with distinct letters are significantly different at $P \leq 0.05$ applying the DMRT test. NT: non-treated HT stressed control, SA 1 (0.5 mM), SA 2 (1.0 mM), SNP (0.5 mM), SA + SNP 1 (0.5 + 0.5 mM) and SA + SNP 2 (1.0 + 0.5 mM).

the exogenous application of SNP (0.5 mM) alone had relatively lower effect on the expression of all the stress-responsive genes except for *TRX* and *LTP* compared to control. Overall, exogenous application of SA, SNP and their combinations triggered a statistically significant increase in the expression of *DCT, ZFP* and *LTP* genes, where the effect of SA (0.5 and 1.0 mM), SA + SNP (0.5 + 0.5 mM) and SA + SNP (1.0 + 0.5 mM) were superior which enhanced the expression of these genes by 6.5–14.2 % (Fig. 5).

3.9. Data retrieval and phylogenetic analysis

The tBLASTn results revealed putative EST mRNA sequences (NCBI ID: JZ151191.1; query cover 35 % and 84 % identity; E-value 1e-97) that encoded the partial HSF02 protein. The sequence (*Lablab purpureus* L.) was further analysed by using BLAST-p programme to find the relevant sequential homologs and orthologues for phylogenetic analysis. The phylogenetic tree constructed based on distance-based UPGMA method showed monophyletic origin of L. *purpureus* with G. *soja (*wild soybean*)* and *G. max* (Fig. 6A). However, the tree constructed based on the maximum parsimony method (Fig. 6B) revealed that L. *purpureus* might more closely evolve from wild soybean, (*G. soja*) (Siebold & Zucc.). The multiple sequence alignment revealed that the functional motif and domain region were found to have minimum divergence across all the evolutionary lineages and had strong conservation of functional residues (Fig. 6C). The maximum conservation of core amino acid residues around N-terminal DNA binding domain of HSF02 indicates the least hindrance might have occurred during phylogenetic evolution. In contrast, the circos analysis revealed conserved genomic positions that encode for the HSF02 protein in L. *purpureus*, *G. max* (NP.001340351.1) and *G. soja* (*KHN04860.1)*. The circos analysis

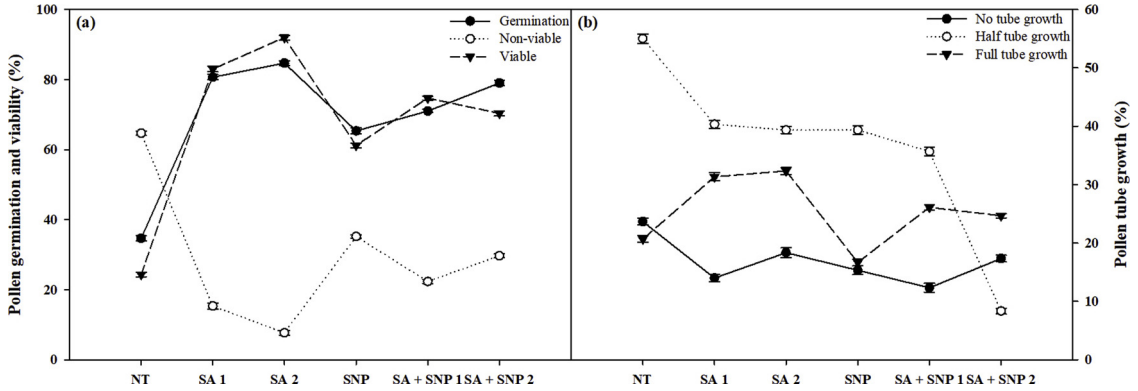

Fig. 3. Aftereffect of different levels of salicylic acid (SA) and sodium nitroprusside (SNP) and their combinations on (a) pollen germination and viability and (b) pollen tube growth in *Lablab purpureus* L (cv VRBSEM-15) under high temperature stress. Mean (± SE) was calculated from three replicates for each treatment. Bars with distinct letters are significantly different at $P \leq 0.05$ applying the DMRT test. NT: non-treated HT stressed control, SA 1 (0.5 mM), SA 2 (1.0 mM), SNP (0.5 mM), SA + SNP 1 (0.5 + 0.5 mM) and SA + SNP 2 (1.0 + 0.5 mM).

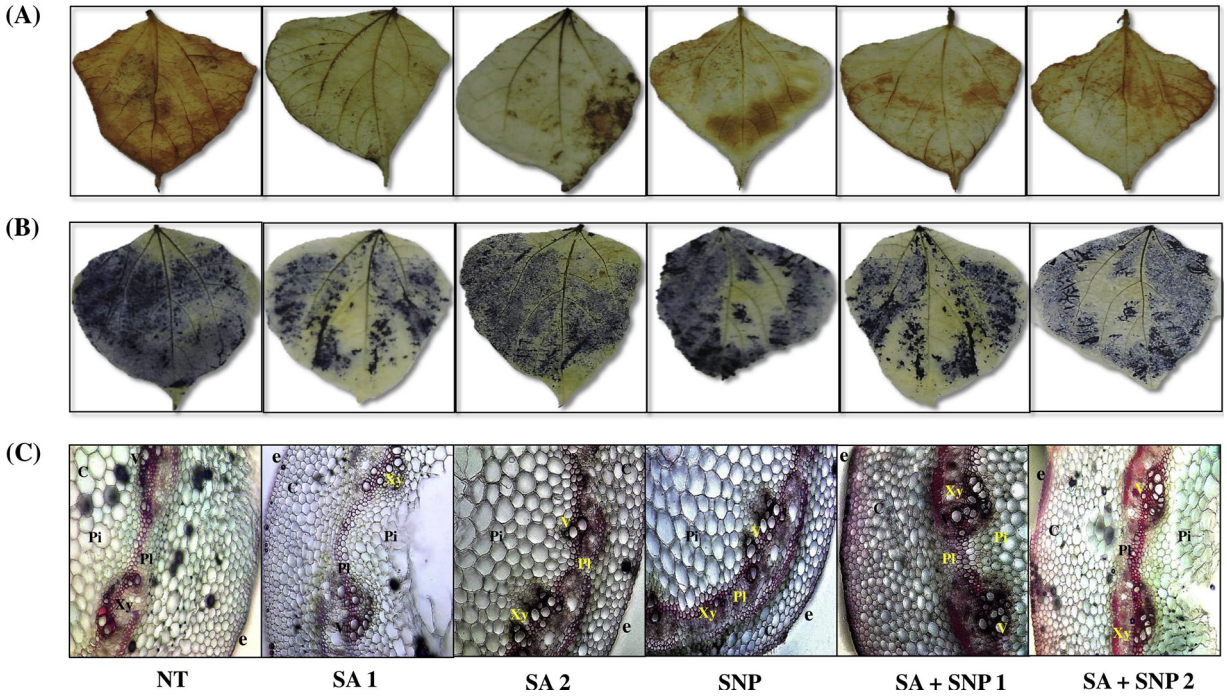

Fig. 4. Aftereffect of different levels of salicylic acid (SA) and sodium nitroprusside (SNP) and their combinations on (a) In-situ accumulation of H_2O_2 by DAB staining (b) $(O_2)^{\cdot}$ anion radicals by NBT staining and (c) changes in cross-sections of stem anatomy in *Lablab purpureus* L (cv VRBSEM-15) under high temperature stress. NT: non-treated HT stressed control, SA 1 (0.5 mM), SA 2 (1.0 mM), SNP (0.5 mM), SA + SNP 1 (0.5 + 0.5 mM) and SA + SNP 2 (1.0 + 0.5 mM).

at lower cut-off filter values depicts the respective relationship of L. *purpureus* with other homolog and orthologous members (Fig. 7). The BLASTp analysis of input and queried sequence against uniprotKB database showed homology with HSF08 (A0A1S3VRV5, identity 91.4 %) of *Vigna radiata*, HSF08 (A0A0B2P6B7, 83.5 %) of *Glycine soja* and HSF08 (A0A151R9Y3, 80.9 %) of *Cajanus cajan* (Supporting information, Fig. S5). Further, phylogenetic tree constructed on BLASTP annotation of uniprotKB also confirmed evolutionary relationship among homologs and orthologs for the predicted protein (Supporting information, Fig. S6).

3.10. Gene prediction and promoter analysis

The tBLASTn results retrieved four significant hits representing the whole genome shot-gun sequences QKRT01000001.1 (query cover 100 %; percent identity 84 %; E-value0.0), PELE01000446.1 (query cover 100 %; percent identity 84 %; E-value 0.0), BBNX02000072.1 (query cover 100 %; percent identity 84 %; E-value 0.0),

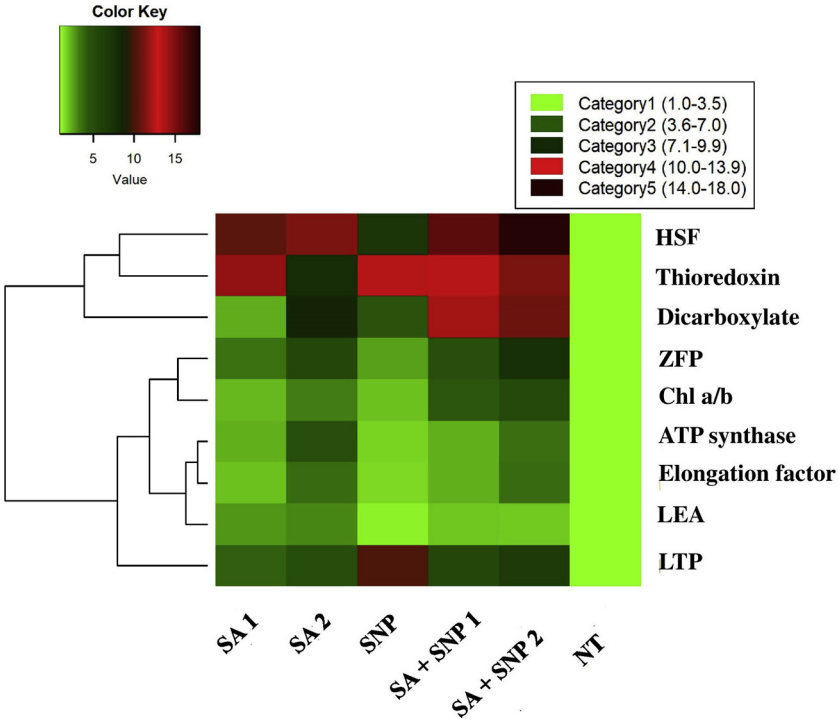

Fig. 5. Heat Map and clustering analysis of stress responsive genes in *Lablab purpureus* L. The rows represent genes while the treatments are shown as columns. The row dendrogram represents the gene clusters with similar pattern. The expression levels are mapped on the colour scale provided at the left top of the figure along with the categories scale on the right. Colour corresponds to the expression level of transcripts with low, intermediate and high expression as represented by green, red and dark red colours respectively. (For interpretation of the references to colour in the figure, the reader is referred to the web version of this article).

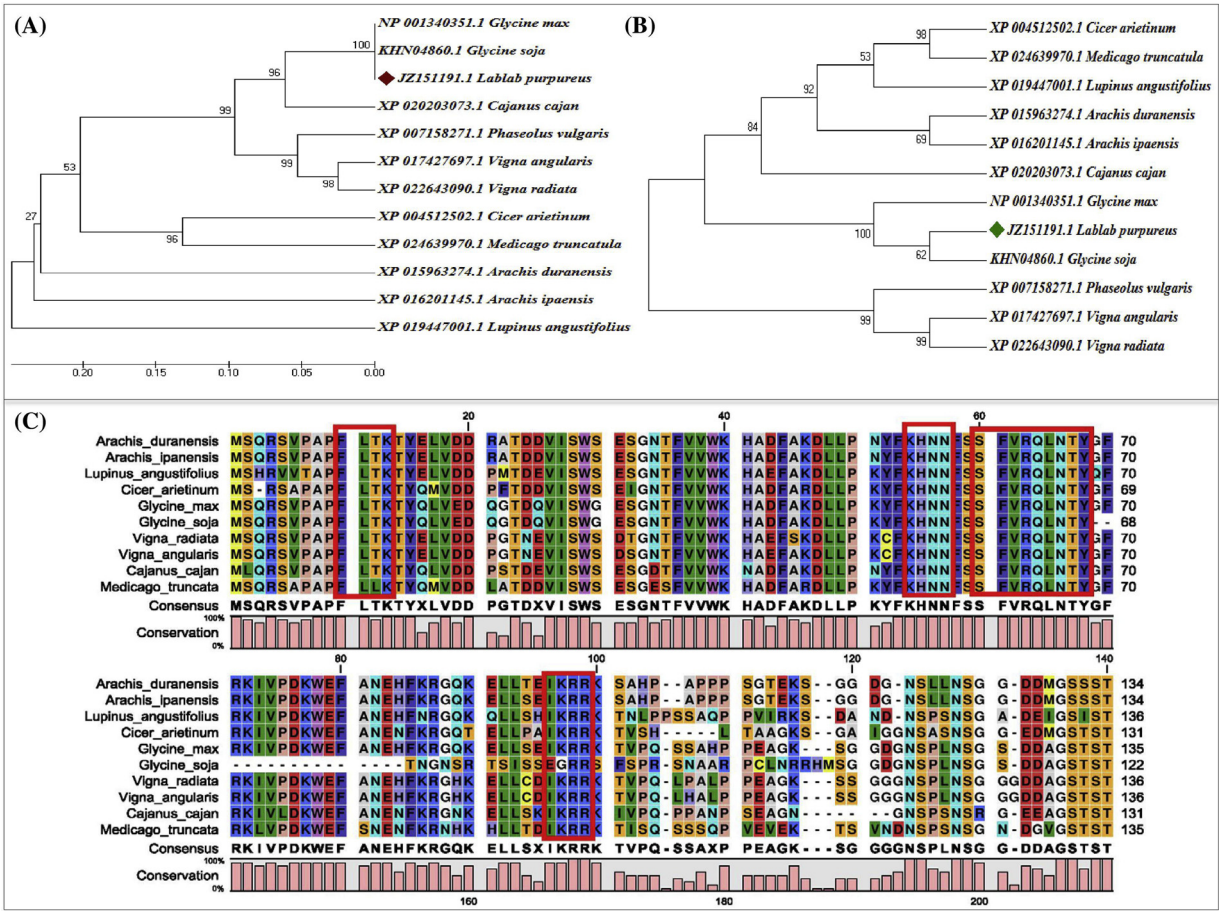

Fig. 6. Phylogenetic tree showing (A) evolutionary relationship and emergence (B) functional homology (C) sequence alignment of the conserved functional domain of heat shock factor protein (HSF02) among different members of legume families. The trees were generated by using 1000 boot replication values based on maximum likelihood methods.

ACUP03000021.1(query cover 100 %; percent identity 84 %; E-value 0.0). The first significant hit was used for finding the CDS region that encodes the HSF02 transcription factor (Supporting information, Fig. S7). The Fgenesh tool revealed the position of TSS, CDS and, PolyA tail region (Supporting information, Fig. S8). The Gene Display server GSDS 2.0 was used for showing the position of TSS, CDS and regions upstream/downstream to TSS. The promoter scan analysis through plant care revealed the position of HSE (-383 bp and sequence 5′AAAAAAT TTC 3′) was lying upstream to the TSS and CDS region that encodes for HSF02. The other promoters lying upstream to the TSS were TCA element (-985 and having sequence GAGAAGAATA) involved in salicylic acid (SA) response, Skn-1 motif (-768; GTCAT), a cis-acting regulatory element required for endosperm expression, TGACG motif (-260; TGACG), cis-acting regulatory element involved in the MeJA response.

3.11. Structural modelling, evaluation and validation

Due to unavailability of experimentally derived (X-ray resolved crystal structure or NMR based solution structure) full length HSF complexed with HSE binding element in plants. The protein sequence HSF02 was searched using PDB advanced search BLAST/PSI BLAST tool. The PDB results retrieved the putative templates with > 90 sequence identity. The significant templates retrieved were 5D5U (Crystal structure of human HSF1 with Satellite III repeat DNA), 5HDN (crystal structure of heat shock factor1-DBD complex), and 5HDG (crystal structure of heat shock factor1-DBD). The first template crystal structure of human HSF1 with HSE DNA having significant hit values with identities: 53/101 (52 %) and positives 70/101 (69 %) was used for retrieval of sequential information for protein homology modelling. The Swiss Modeller server was used for the generation of protein models. Swiss modeller generated three protein models of which the model having better qualitative and quantitative score values were selected for DNA protein interaction studies. The final model generated was further refined to eliminate the loop regions using ModRefiner tool (Fig. 8A and Table 4). The final refined model was submitted to Protein Modelling Database (PMDB), an online repository database which assigned the model with a with accession identity (PM0081630). The DNA sequence (5′AATAAATTTC 3′) specific to heat shock element (HSE) were retrieved through Plant care promoter database (Fig. 8B) was modelled using DNA sequence to structure tool available at http:/www.scfbio-iitd.res.in/software/drugdesign/bdna.jsp (Arnott et al. 1976).

The Ramachandran plot analysis of initial (before refinement) and final (after refinement) models through RAMPAGE server revealed percent residue in the favoured and allowed regions were 98 % and 2.0 % in initial model while in the final model the percent residue in the favoured and allowed regions were 98.9 % and 1.1 % (Table 4). The results of Volume, Area, Dihedral Angle Reporter (VADAR) analysis further confirmed the topological confirmation of both initial and final models which further confirmed the helix type structures of both initial the models as predicted by the CATH server. The VADAR results for initial model have observed values of 39 (43 %) helix, 20 (22 %) beta, 31 (34 %) coil and 20 (22 %) turns with mean H bond energy (-1.4 SD = 1.1) against the expected values of -2.0 (SD = 0.8). In contrast, for the final (refined) model we observed lowest deflation for the above parameters i.e. observed values of 32 (35 %) helix, 19 (21 %) beta, 39 (40 %) coil and 36 (40 %) turns with mean H bond energy (-1.3 SD =

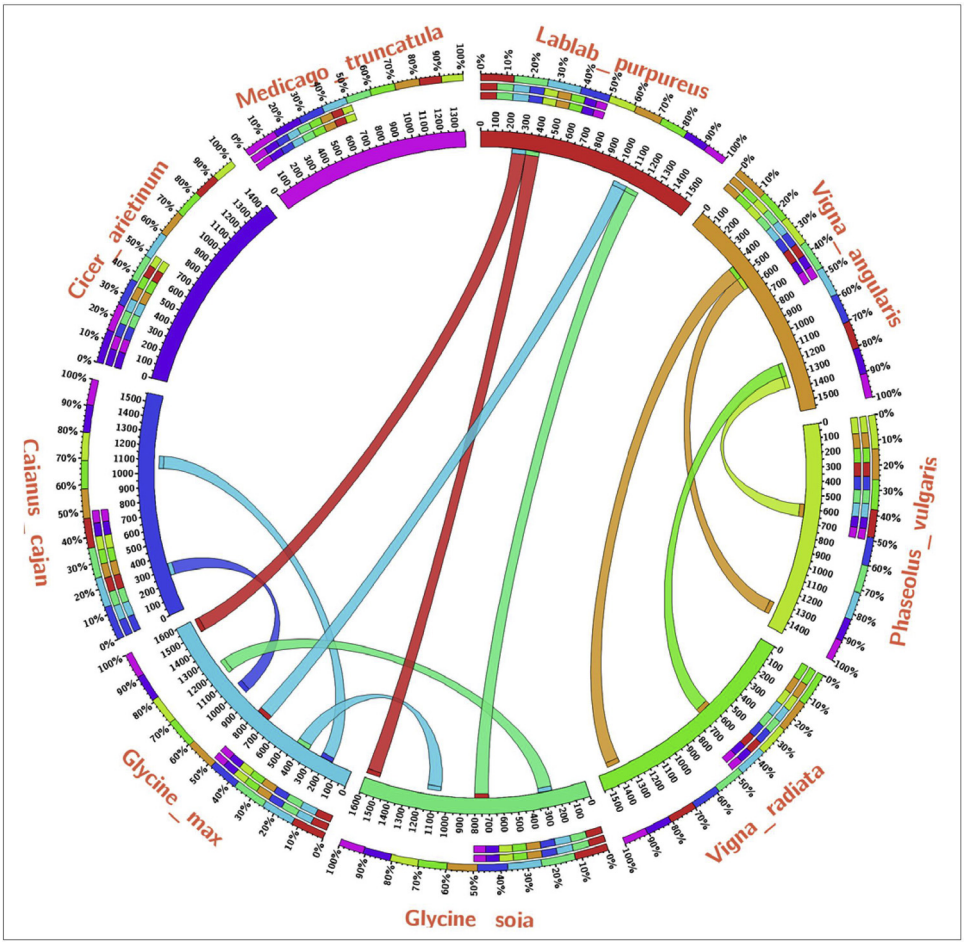

Fig. 7. Comparative analysis of similarities and differences in heat shock factor protein (HSF02) among different members of legume family. The Circos software was used to generate circular map based on similarity percentage matrices using Clustal W algorithm.

0.9) against the expected values of -2.0 (SD = 0.8).

The modelled proteins were further validated and verified qualitatively by using PROCHECK analysis (Fig. 9A) and it was observed that both these models contained 91.4 % residues in the most favoured regions (A, B, L) with 8.6 % additionally allowed residues (a, b, l, p). However, good quality proteins models are generally considered to have more than 90 % residues in the most favoured region. Additionally, ProSA server was used to analyse errors in both the predicted models by evaluating z-scores (Fig. 9B). The results of ProSA confirmed that the stereo-chemical properties of predicted models are reliable

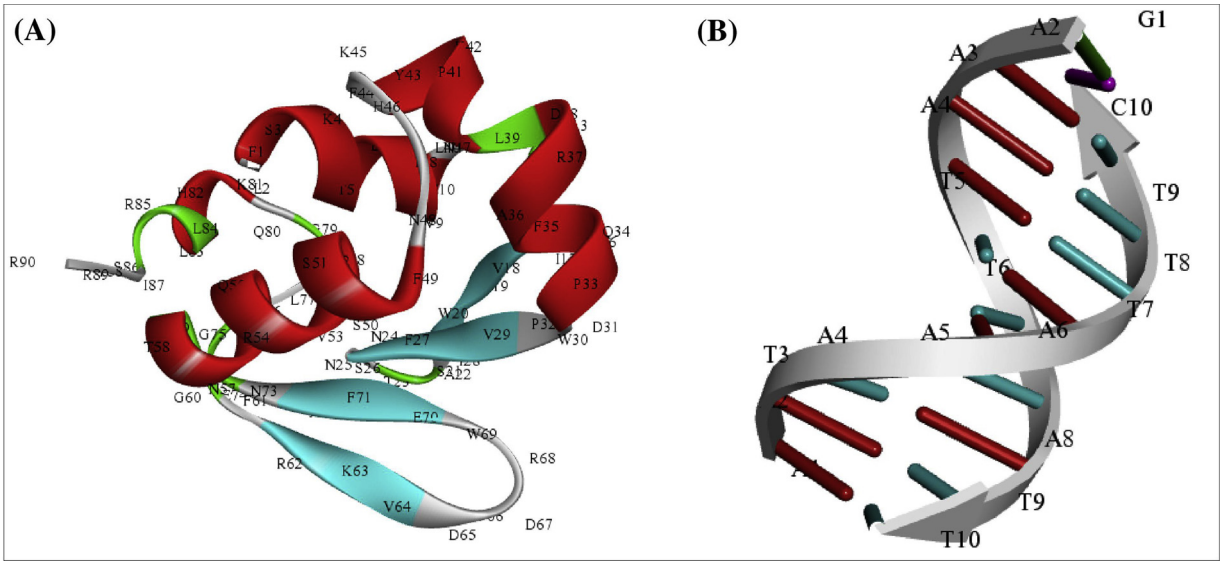

Fig. 8. Predicted structures of (A) functional domain of HSF02 visualized by swiss modeller (B) structure of the heat shock element (AATAAATTTC).

Table 4
Comparative qualitative and quantitative analysis of predicted/modelled protein HSF02, 5D5U (template 1), 5HDG (template 2) and 5HDN (template 3).

S. No.	Protein name	Qmean score	Z score	Overall quality factor score	Errat	ReSProx	RAMPAGE results		
							Most favoured (%)	Additional allowed (%)	Outlier region (%)
1.	HSF02 Heat shock transcription factor *Glycine max* (NCBI ID: NP.001340351.1) (before refinement)	−1.87	−5.74	80.24		1.174	98.0	2.0	0.0
2.	HSF02 Heat shock transcription factor *Glycine max* (NCBI ID: NP.001340351.1) (after refinement)	−1.30	−6.00	80.48		1.225	98.9	1.1	0.0
3.	Crystal structures of human HSF1 with HSE DNA (PDB ID: 5D5U) (Template protein 1)	−1.39	−3.78	98.43		1.337	91.7	8.3	0.0
4.	Crystal structure of HSF1-DBD (PDB ID: 5HDG) (Template protein 2)	0.01	−4.90	98.36		1.409	97.8	2.2	0.0
5.	Crystal structure of HSF1-DBD complex (PDB ID: 5HDN) (Template protein 3)	0.45	−3.91	100		1.296	96.9	3.1	0.0

Both predicted and modelled structures were compared with X-ray analysed structures. Proteins with ReSProx value (0–1.5) is considered as good quality protein.

(Fig. 9B). Further, Qmean and RESPROX evaluate the reliability of models in terms of geometrical and atomic resolutions. The predicted models were also subjected to verify 3D server to analyse their 3D profile and revealed that in our predicted structures, 98–100 % of the residues have averaged 3D-1D score ≥ 0.02 values as compared to templates proteins that had an average of 5D5U (61.1 %), 5HDG (62.1 %) and 5HDN (69.8 %) residues covering 3D-1D score ≥ 0.02. All the above qualitative and quantitative parameters confirmed the stability, reliability and quality of our modelled structures.

3.12. DNA protein interaction

The DNA-protein interaction was performed using the modelled protein with DNA (HSE) using Hex Docking server. The DNA protein interaction study revealed ten docked conformational structures. The docked complex having minimum interaction energy (most stable) was selected further for visualization through Discovery studio 3.0 visualizing tool. In our results, we found that the interaction energy for the most stable complex was E total = -1140.56 KJ/M. All the probable amino acid residues involved in the interaction with HSE motif in HSF02 as well as in the templates proteins have been highlighted in Fig. 10A. Docking studies revealed that the key residues Phe^{21}, Leu^{22}, Ser^{23}, Lys^{24}, Lys^{65}, His^{66}, Asn^{67}, Ser^{71}, Arg^{74}, Gln^{75}, Thr^{78}, Tyr^{79}, Leu^{103}, Arg^{104}, Ile^{105}, Thr^{106}, and Arg^{107} were involved in the interaction of HSF02 with HSE motif (AATAAATTTC) sequence (Fig. 10B).

3.13. Protein-protein interaction network

The STRING server was used to find possible protein-protein interaction partners. The results revealed that the model protein was found to be in interaction with (heat shock protein 90 kDa beta, GLYMA09G16690.1 (0.812), (heat shock protein 90 kDa beta, GLYMA17G37820.1) (0.812) and HSF90-1 (0.768) (Fig. 11A) with maximum interactions score values at highest confidence level from both shell of interactors. The lablab homologues for GmHSF02 was also found in interaction (Fig. 11B) with heat shock protein 90 kDa beta (GLYMA09G16690.1, score value 0.812), heat shock protein 90 kDa beta (GLYMA14G40320.1, score value 0.812) and lastly by heat shock protein 83-like (GLYMA16G29750.1, score value 0.768). These data suggested that conserved protein have similar functions across the distant evolutionary lineages. One important conclusion that could be deduced from such interaction analysis was both *G. max* and L. *purpureus* utilizes the same interaction partner sharing similar functional mechanism and signalling cascades to mitigate the different environmental stresses and therefore, predicted their integrative and regulative function to encounter various challenges for a better adaptation of plants to stress conditions. The interaction partners with their interaction score and identities have been tabulated in Supporting information, Tables S2 and S3.

3.14. Gene ontology analysis

The functional annotation of model proteins was further investigated based on gene ontology (GO) enrichment analysis, structured around three ontologies including biological process, molecular function and cellular location. Further, the subcellular localization and functional annotation were confirmed using CELLO2GO web server. The results of ReviGO analysis were depicted in terms of scatter plot diagram in which significant GO terms were indicated by unique colours based upon their biological processes and molecular functions (Fig. 12). The ReviGO analysis revealed all the significant gene ontologies relevant to the HSF02 protein. The first five significant GO terms associated with the submitted protein were involved in biological processes in response to osmotic stress (GO:0,006,970), heat acclimation (GO:0,010,286), regulation of cellular response to heat (GO:0,009,408), protein phosphorylation (GO:0,006,468) and defence

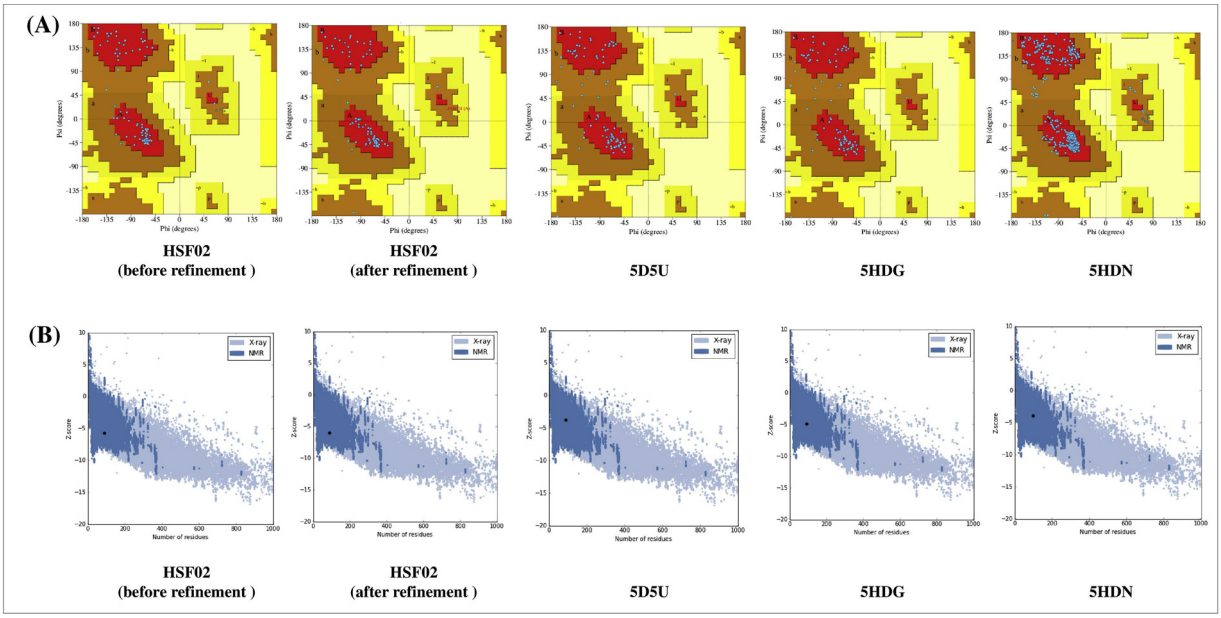

Fig. 9. Qualitative analysis of predicted model using PROCHECK and ProSA analysis. (A) The stereo chemical spatial arrangement of amino acid residues in predicted model (before and after refinement) were compared with experimentally resolved structures (5D5U, 5HDG and 5HDN) through PROCHECK server. Most favoured regions are coloured red while additionally, generously and disallowed regions are indicated with yellow, light yellow and white fields respectively (B) Qualitative estimation by ProSA server, that measures structural errors in each amino acid residues. (For interpretation of the references to colour in the figure, the reader is referred to the web version of this article).

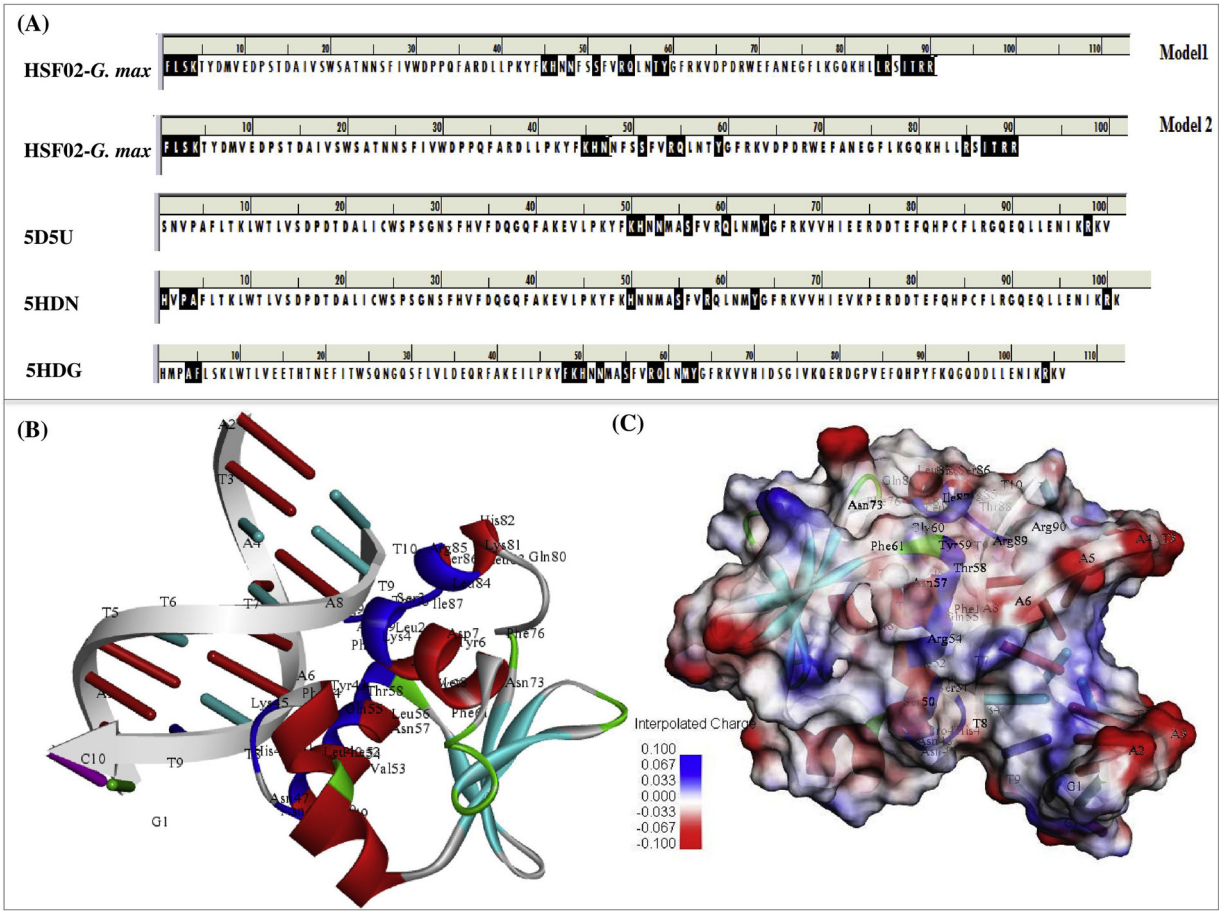

Fig. 10. (A) Comparative analysis of docked complex with experimentally resolved X-RAY diffraction structures of functional domain of 5D5U, 5HDG and 5HDN with HSE motif. The residues PAFKHNRQMY made interaction with HSE motif compared to our predicted complex where FLSKKHNRQTY with initial flanking sequence were involved in interaction with HSE motif (B) Structure of docked complex (HSF02 with HSE motif) as visualized Discovery Studio 3.0 (C) Three-dimensional surface view for HSF02-DNA interaction highlighting the docked complex in terms of interpolated charge in docked complex.

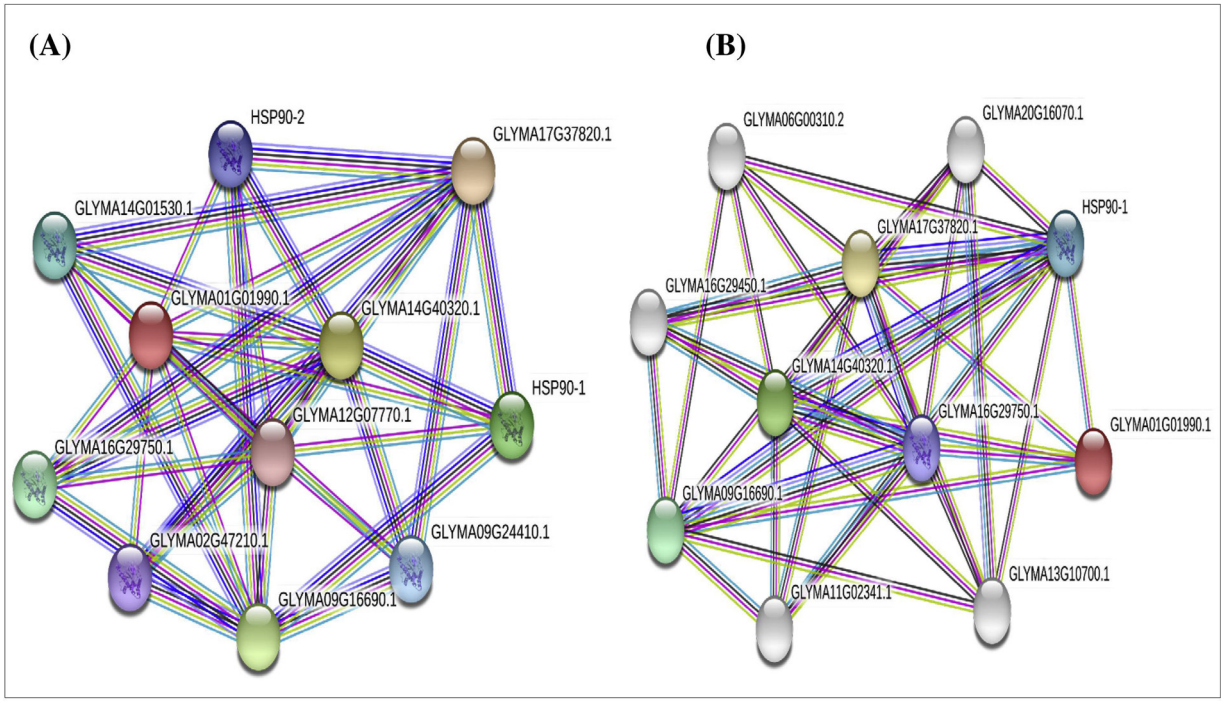

Fig. 11. Functional interactive network of (A) GmHSF02 and (B) lablab homolog of GmHSF02 with other protein family members as found on STRING server where the coloured nodes describe query proteins from first shell interactors and white nodes are form second shell interactors.

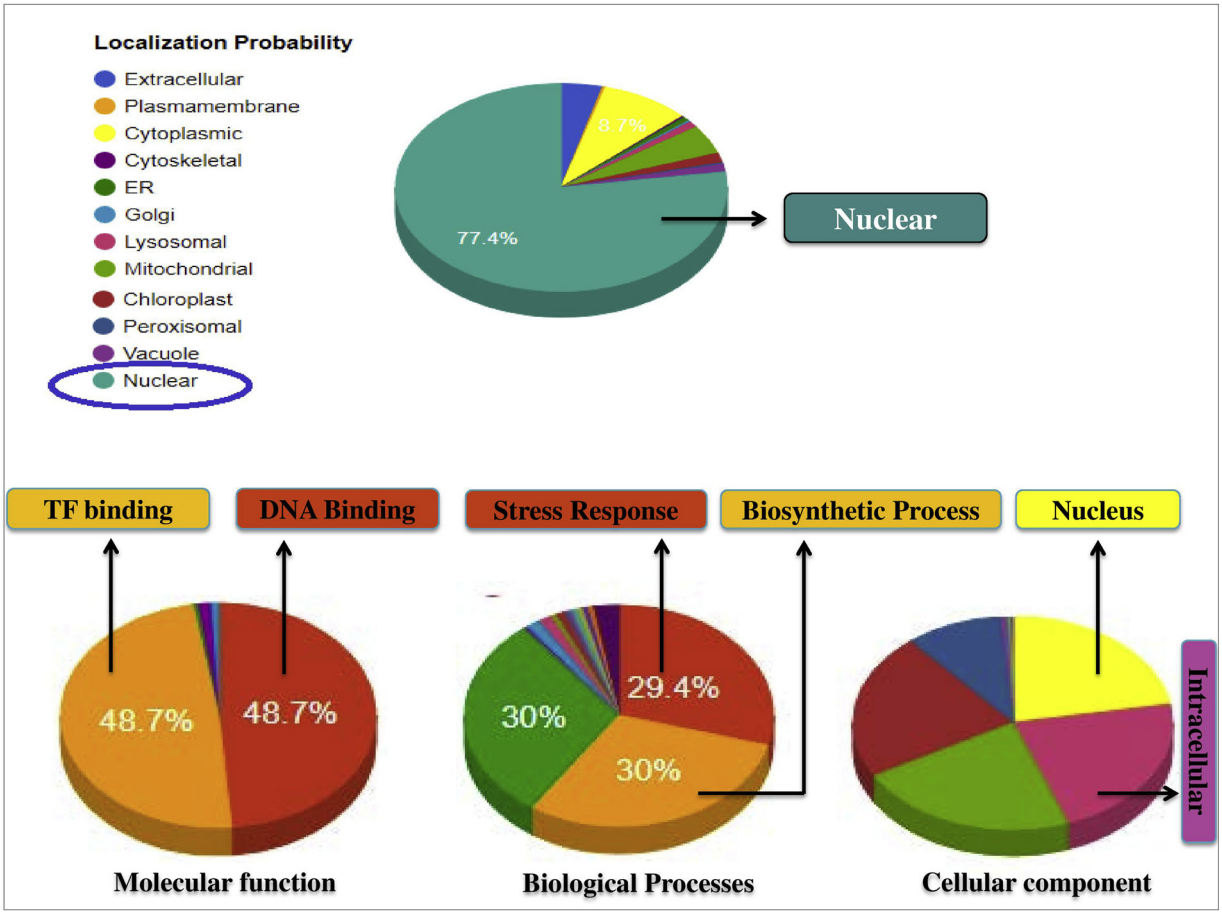

Fig. 12. The subcellular localization and functional gene annotation using CELLO2GO web server. The significant terms are represented in terms of their percentage contribution.

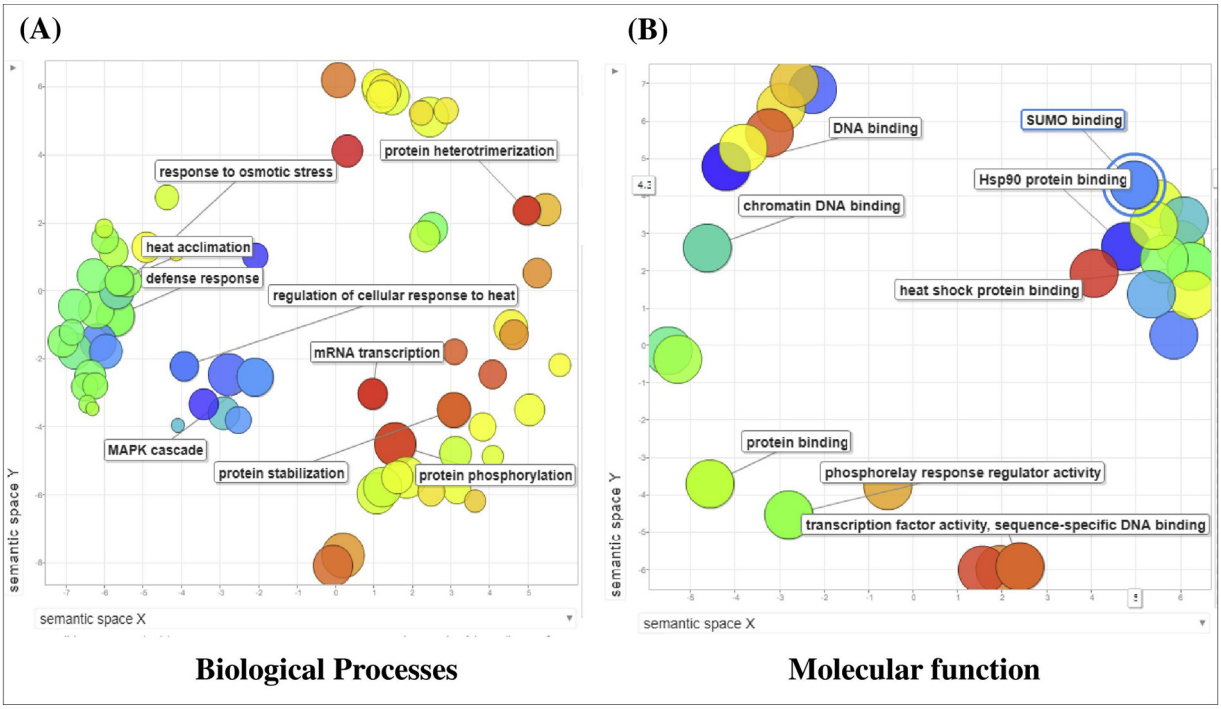

Fig. 13. Gene ontology analysis using ReviGO web server. The functional and significant GO terms involved in (A) biological processes and (B) molecular function are shown on scattered plot diagram using hypergeometric test distribution.

response (GO:0,006,952). Additionally, the significant terms involved in molecular functions were DNA binding (GO:0,003,677), HSP90 protein binding (GO:0,051,879), heat shock protein binding (GO:0,031,072), SUMO binding (GO:0,032,183) and chromatin DNA binding (GO:0,003,682). The CELLO2GO results confirmed that the 77.4 % of HSF02 protein was located in the nucleus (with maximum score value of 3.94) involved in transcription factor DNA binding activity (48.7 %), biosynthetic process (30 %), cellular nitrogen metabolism process (30 %) and in stress management response (29.4 %) (Fig. 13).

4. Discussion

Salicylic acid and nitric oxide are involved in the regulation of various plant growth and developmental processes including germination and immune responses under various abiotic stresses such as high temperature, salt, drought and metal toxicity (Hasanuzzaman et al., 2017; Rai et al., 2018c). In the present study, morpho-metrical attributes such as photosynthetic photon flux density, chlorophyll colour index, Fv/Fm, the number of pods per plant and yield per plant were gradually reduced in non-treated control plants upon exposure to HT stress (Table 1). However, foliar application SA + SNP (0.5 + 0.5 mM) and SA + SNP (1.0 + 0.5 mM) more effectively alleviated the negative effect of HT stress and improved the growth, photosynthesis and yield of L. *purpureus* L. plants compared to individual applications of SA and SNP (Supporting information, Fig. S1). Studies have reported that both SA and NO show synergistic or antagonistic relation in the regulation of plant processes, where NO can stimulate the endogenous level of SA that may have triggered the signalling networks involved in regulation of plant physiological process such as photosynthesis, production of osmolytes which may have improved the growth and yield of L. *purpureus* L plants (Manjunatha et al., 2010). Our results are in consistent with the findings of Nazar et al. (2015) and Hasanuzzaman et al. (2013) indicating lower concentrations of SA and SNP improves morpho-physiological attributes of plants while higher concentrations had a negative impact on their growth and productivity.

The decrease in chlorophyll and carotenoid content in HT stressed L. *purpureus* L plants in the present study might be due to the possible oxidation of chlorophyll and other pigments due to the generation of osmotic stress induced by decreased relative water content and CO_2 availability resulting in the excess ROS formation in chloroplast and closing of stomata (Rai et al., 2017). The HT stress induced chlorophyll degradation and water loss was significantly reversed more efficiently in the L. *purpureus* L plants treated with SA + SNP (0.5 + 0.5 mM) and SA + SNP (1.0 + 0.5 mM) compared to their corresponding counterparts (Table 2). The improvement in the photosynthesis and enhancement in the plant relative water content in SA + SNP treated plants may be due the positive interaction of NO with the SA signalling pathways that may have facilitated increased chlorophyll synthesis and water content for improving plant HT stress tolerance (Tada et al., 2008). Several studies have delineated the stimulatory effect of SA and SNP in conferring abiotic stress tolerance in plants by regulating photosynthesis, reducing membrane damage and maintaining adequate leaf water potential (Zhang et al., 2011; Khan et al., 2012; Hasanuzzaman et al., 2012) which are in accordance with the result of the present study.

Hydrogen peroxide and superoxide anion production were markedly increased in HT stressed L. *purpureus* L plants (Table 3; Figs. 4a,b and S3). In the present study, application of SA (1.0 mM), SA + SNP (0.5 + 0.5 mM) and SA + SNP (1.0 + 0.5 mM) significantly and efficiently contrived HT induced oxidative burst in *Lablab purpureus* L plants compared SA and SNP alone (Table 3). The SA and SNP induce reduction in ROSs level may be due to the SA induced NO production by stimulating nitrate reductase activity, that limits HT-induced oxidative damage thereby acting as a potent scavenger of ROSs under abiotic stresses. The collaborative function of NO and SA in scavenging of ROS and their modulation in signalling process have been reported in *Arabidopsis*, where SA-induce NO production efficiently control the ROSs generation in guard cells by activating antioxidant defence system (Khokon et al., 2011). Lipid peroxidation and electrolytic leakage are one of the most common indicators of oxidative stress, that occurs when the ROSs level exceed beyond the capacity of antioxidant defence system (Wang et al., 2010). In the present study, the effect of HT induced membrane damage (Table 3) in L. *purpureus* L plants was

markedly reduced by the foliar application of SA + SNP (0.5 + 0.5 mM) and SA + SNP (1.0 + 0.5 mM). The decrease in the membrane damage could be due to increased accumulation of proline in SA + SNP treated L. *purpureus* L plants subjected to HT stress (Table 3) which may in turn have strengthened membrane integrity, stabilize enzymes/proteins and promoted the scavenging of free radicals (Rai et al., 2015, 2016).). Foliar application of SA and SNP at low concentrations has been documented to stabilizes membrane integrity by regulating the osmotic balance, electrolytic leakage and scavenging of reactive oxygen species (Wang and Li, 2006; Ashraf and Foolad, 2007; Khan et al., 2012; Hasanuzzaman et al., 2012).

The enzymes of Halliwell-Asada pathway *viz.,* DHAR, MDHAR, APX, GR along with CAT and SOD together with vital components AsA and glutathione are actively and readily involved in the detoxification of ROSs (Rai et al., 2018a). In the present study, the activities of all the enzymes increased upon the application of SA and SNP in HT stressed L. *purpureus* L plants (Figs. 1 and 2). The ameliorative effect of combined SA and SNP treatment and induction of antioxidative defence system in L. *purpureus* L plants could have resulted in reduce accumulation of ROSs by modulating Ca^{2+} signalling as second messenger, which in turn may have led to the induction of antioxidant defence machinery and consequent changes in different biochemical and physiological parameters thereby strengthening plants performance under HT stress (Fan and Liu, 2012). Our results are in the accordance with the results of previous studies of Janda et al. (1999); Hasanuzzaman et al. (2013); Khan et al. (2014) and Nazar et al. (2015) where they have corroborated that exogenous application of SA (0.5 and 1.0 mM) and SNP at lower concentrations modulated the levels of antioxidant enzymes such as APX, GPOX and SOD which in turn improved photosynthesis and growth and survival of *Z. Mays, V. radiata* under HT stress and *B. juncea* to salinity stress.

The development of viable pollen grains, successful pollen germination and efficient pollen tube growth for lucrative pollen-pistil interaction are pre-requisites for ovule fertilization and seed development (Jimenez-Quesada et al., 2017). To the best of our knowledge, not much of the report is available on the effect of SA and SNP on pollen germination and viability under HT stress. In the present study, foliar application of SA + SNP combination mitigated the adverse effect of HT stress and improves the viability, germination and tube growth of the pollen grains by 61.3–92.5 % (Fig. 3 and Supporting information, Fig. S2). A direct relationship between viable pollen grains and germination percentage has occurred in L. *purpureus* L plants which may be due to the synergic effect of SA and NO on cGMP degradation, a secondary messenger that has been known to regulate pollen viability, germination and tube growth (Jimenez-Quesada et al., 2017). Similar findings have also been reported by Hussain et al. (2009) where they have indicated the exogenous application of salicylic acid and glycine betaine at lower concentration significantly improved pollen germination in drought exposed sunflower plants.

HT stress significantly increased the cortex diameter and decreased the diameter of xylem/phloem cells in non-treated control plants (Fig. 4c and Supporting information, Fig. S4). Foliar applications of SA, SNP and their combinations significantly improved the number and diameter of xylem, phloem, vessels and limits the diameter of the cortex in L. *purpureus* L. plants under HT stress. The results obtained in the present study showed fine modulation of NO-induced SA synthesis might have fine-tuned the physiological development of cellular components i.e. cortex, xylem and phloem by lowering disruption of cytosolic Ca^{2+} gradient and concomitantly maintaining appropriate pH at cytological level (Wang et al., 2015). Very few reports are present on the effect of SA and SNP regarding their role in strengthening xylem and phloem vessels diameters under HT stress conditions. However, Hasan et al. (2018) demonstrated that exogenously applied SA significantly improved vascular bundle thickness in *Viccia faba* plants exposed to salinity stress results of which are in accordance with the observations of present study.

Expression of key stress-related genes in L. *purpureus* L. plants were analysed by RT-PCR under HT stress. The results showed that the expression levels of genes were generally high in the plants treated with SA + SNP compared to SA and SNP alone (Fig. 5). In the current study, the maximum expression of *ZFP* gene was observed for SA (0.5 and 1.0 mM) and combined SA + SNP treatments. Zinc finger proteins (*ZFPs)* belongs to the largest family of transcriptional regulators that are involved in the regulation of key cellular processes and also has been known to enhance the ROSs scavenging antioxidant enzymes under stress conditions which result in the increased tolerance of plants (Wang et al., 2015). Enhanced chlorophyll and carotenoid content were observed in the plants treated with SA + SNP and SA (1.0 mM) which may be due to differential effect of SA, SNP and their combination on the expression of Chl a/b genes (Fig. 5) in *Lablab purpureus* L. plants exposed to HT stress.

Overexpression of *LEA*, *ATP synthase* and elongation factor genes were also observed in the plants treated with SA + SNP and SA (1.0 mM) indicating that these genes could be regulated in *Lablab purpureus* L. plants under HT stress (Fig. 5). The over-expression of *LEA* genes, *ATP synthase* genes and *elongation factor* genes has been shown to enhance drought tolerance in rice and poplar plants by mediating some physiological and biochemical process, as we observed in the present study (Xiao et al., 2007; Gao et al., 2013). The expression of *LTPs* and dicarboxylate genes was differentially regulated in HT stressed *Lablab purpureus* L. plants treated with SA, SNP and their combinations suggesting their role in mitigating HT induced oxidative stress (Federico et al., 2005; Wang et al., 2009). Concentration-dependent application of SA and SNP have been shown to stimulated the expression of several genes involve in stress defence response thereby mitigating the adverse effect of abiotic stress induced oxidative damages in several plant species (Csiszar et al., 2014). For instance, foliar application of SA and SNP have been reported to ameliorate the adverse effect of salt and drought stress in *Triticum aestivum* and *Z. mays* by over-expressing certain stress responsive genes as well as level of stress defence pathway enzymes (Saruhan et al., 2012; Hasanuzzaman et al., 2013; Kang et al., 2013; Li et al., 2013).

The expression of *HSF* gene was shown to be upregulated upon the application of SA, SNP and more prominently in SA + SNP combinations (Fig. 5). The increase in the expression of HSF might be due to SA induced activation of protein kinase that functions in the refolding/transport of antioxidant proteins to the mitochondria (Wang et al., 2004b; Cruz de Carvalho, 2008). Thioredoxin h (*Trx h*) are involved in the regulation of crucial biological processes such as germination, seedling growth and are also involved in the cellular protection against abiotic stresses (Cazalis et al., 2006). In the present study, differential and higher expression of *Trx h gene* were observed in SA + SNP treated HT stressed L. *purpureus* L. plants proving that SA and SNP combination can induce HT stress mediated molecular response. Furthermore, overexpression *Trx h* gene may be the reason behind the improve pollen viability, germination and tube growth of *Lablab purpureus* L. plants under HT stress (Lee et al., 2005).

To deduce the evolution of HSF family transcription factor among different members of the legume family, we constructed a phylogenetic tree based on UPGMA and maximum parsimony methods. UPGMA based phylogenetic investigation revealed monophyletic origin of EST-based lablab HSF02 homolog with *Glycine max HSF02*, *Glycine soja HSF02* and close relationship with *Cajanus cajan HSF02,* whereas *Phaseolus vulgaris HSF02*, *Vigna radiata HSF02* and *Vigna angularis HSF02* showed paraphyletic relationship with lablab HSF02 (Fig. 6A). In contrast, phylogenetic analysis based on maximum parsimony revealed the monophyletic origin of EST-based lablab HSF02 homolog with *GsHSF02* and closer relationship between lablab HSF02 and *GmHSF02* (Fig. 6B). Yao et al. (2013) also observed a similar level of sequence homology between L. *purpureus* L and *G. max* for MYB transcription factor. In their study, they created Suppression subtraction hybridization (SSH) libraries against drought stress and generated 1287

unigenes (derived from sequence alignment and cluster assembly of ESTs). The result of BLASTx against NCBI non-redundant database revealed 61.5 % homology with *G. max* and 1.44 % close similarity with *P. vulgaris* respectively. The result of MSA revealed strong conservation and least disturbances of amino acid residues around the DNA binding domains (Fig. 6C). The interaction of these evolutionarily conserved amino acid regions with specific ligands has shown to trigger defence response under changing environments (Vihervaara et al., 2013; Jaeger et al., 2016).

Comparative genomic analysis reveals 61.5 % sequence homology between *Lablab purpureus* L. and *G. max* and *G. soja.* Interestingly, functional annotation and cataloguing of ESTs database have also confirmed the similarity between L. *purpureus* and *G. max* (Yao et al., 2013), which has also been observed in our results through phylogenetic (Fig. 6A and 6B and Circos analysis (Fig. 7). The results of this comparative genomic analysis can be used to retrieve information from *G. max* genome for further understanding of the functional divergence and evolution of HSFs proteins in several other non-sequenced crops *per se*., L. *purpureus* L. Furthermore, this functional homology could also be employed to understand other interactive functions of HSFs as they are also reported to regulate the signalling pathway of other stress-responsive transcription factors/genes such as DREB, WRKY and MYB under several abiotic stress conditions (Ma et al., 2015).

Predicted L. *purpureus* HSF02 protein models were found congenial as ascertained by their qualitative and quantitative assessments and were very much alike with template proteins (Fig. 8A). Analysis of protein 3D structures stipulate significant insight into its molecular function and facilitate the identification of putative active site residues (Madej et al., 2014). Furthermore, structural and functional characterization of proteins can also reveal important information about the conformation, stability and specific binding of HSF proteins with HSEs which is required for its cellular and biological functions under stress condition (Wang et al., 2017). The RAMPAGE statistics for the predicted HSF02 model showed that the % of residues in the core region and allowed regions were 98.9 % and 1.1 %, and the red shading on the plot correspond to the core region delineating significant combinations of φ and ψ values (Fig. 9A). The appearance of more than 90 % residues of protein in core regions is the indication of its good stereochemical quality (Vatansever et al., 2016.). The result of PROCHECK analysis reveals 0.0 % protein residues in disallowed regions suggesting the reliability of predicted L. *purpureus* HSF02. Recently, analysis of stereochemical qualities of modelled LeNRAMP proteins and WRKY proteins through *in-silico* approach have also been elucidated in tomato plants (Aamir et al., 2017; Meena et al., 2018), which corroborates the results of the present study.

Heat shock elements are palindromic repetitive motifs (5′-AGAAnnTTCT-3′) which is known to interact with heat shock transcription factors, located upstream of TATA box of the promoter region which is essential for growth and survival of plants under abiotic stress conditions (Neudegger et al., 2016). In the present study, the docked complex of HSF02 and HSE motif has E_{total} = -1140.56 KJ/M. Several researchers have reported that complexes having low binding energies (most negative value) indicates efficient interaction between protein and ligand and also contribute to the stability of the docked complexes (Ritchie, 2003; Antony et al., 2012). Additionally, the docking study revealed that the key residues Phe^{21}, Leu^{22}, Ser^{23}, Lys^{24}, Lys^{65}, His^{66}, Asn^{67}, Ser^{71}, Arg^{74}, Gln^{75}, Thr^{78}, Tyr^{79}, Leu^{103}, Arg^{104}, Ile^{105}, Thr^{106}, and Arg^{107} were involved in the interaction of HSF02 with HSE motif (AATAAATTTC) sequence (Fig. 10B). Furthermore, the results indicated that HSF02 binds with cis-regulatory DNA sequence through conserved FLSKKHNRQTY residues of helix-turn-helix motifs where Phe, Leu, Ser, lys, Ala, Cys and Thr are crucial for maintaining the stability of DNA-protein complexes (Kotak et al., 2007; Akerfelt et al., 2010). Role of signalling molecule such as nitric oxide (NO) in the activation of heat shock transcription factor has been visualized by Xu et al. (Xu et al., 1997), where they have reported NO mediated induction of HSP70 protein.

The protein-protein interaction results predicted for GmHSF02 and GmHSF02 homologues for L. *purpureus* manifested similar types of functional interactive network, which was also confirmed by the study of Yao et al. (2013) that L. *purpureus* L. shares maximum sequence homology with *G. max*. The identification and characterization of conserved proteins through interactive networks can be employed for the identification of probable genes involved in biological processes and possible interaction that might exist with other orthologous or paralogues members with in the same family (Sun and Kim, 2011). Gene ontology study of predicted L. *purpureus* HSF02 using ReviGO clustering analysis reveals response to osmotic stress, heat acclimation and defence response among most upregulated biological processes whereas SUMO binding, HSP90 protein binding and chromatin DNA binding among the most expressed molecular functions (Jiang and Deyholos, 2009). The members of HSP family have been reported to function as molecular chaperones involved in maintaining protein homeostasis and SUMO DNA binding has been shown to engage in enzymatic and non-enzymatic antioxidants (Hietakangas et al., 2003). Overall, the gene ontology analysis of the modelled HSF02 protein of *G. max* homolog of L. *purpureus* L. in the present research revealed significant insight on its biological and functional properties which could provide valuable information regarding its regulatory mechanisms under abiotic stress conditions.

5. Conclusion

The results obtained in the present study elucidate that both salicylic acid and nitric oxide execute important functions in the modulation of physiological and biochemical defence response in lablab plants exposed to HT stress. The results concluded that foliar application of combined SA and NO were effective in ameliorating HT induced oxidative stress in lablab plants by regulating pollen viability and germination (up to 80 %). It also enhanced the accumulation of proline by 1.0 % and also significantly contrived the generation of ROS by stimulating the activities of antioxidant enzymes (60–150 %) and by modulating the expression of stress-responsive genes (7–18 %). *Lablab purpureus* L. pod yield was also significantly increased by 50–110 %. The results of *in-silico* analysis reconciled with our experimental hypothesis and gave valuable insight into structural and functional properties of heat shock transcription factors (HSFs) and confirmed that this strategy could provide a better understanding of specific functions of plant HSFs in transcriptional reprogramming of stress-responsive genes. However, further in-depth research about the transcription factors is required to define their functional mechanism responsible for the fine-tuning of gene expression regulation under stress conditions.

6. Compliance with ethical standards

Conflict of interest: The authors declare no conflicts of interest.

7. Author's contributions

K.K.R., planned and conducted all field and *in-vitro* experiments, *in-silico* analysis, wrote final draft of the manuscript; N.R., provided the materials and supervised the work; M.A., performed all the *in-silico* analysis and assisted in the interpretation of *in-silico* results; D.T., assisted in histochemical experiments and statistical analysis., S.P.R., designed, planned and supervised the whole work, prepared final draft of the manuscript.

8. Declaration of Competing Interest

The authors declare no conflicts of interest.

Declaration of Competing Interest

The authors report no declarations of interest.

Acknowledgements

The authors are thankful to the Director, Indian Institute of Vegetable Research, Varanasi for providing necessary funds and facilities for conducting the research. The authors are also thankful to DST (Department of Science and Technology), Govt. of India (Grant No. DST/BHU/PURSE 2017-18 and DST/BHU/FIST 2016-17) for financial support and central facility of the department to carry out functional genomics work in BHU, Varanasi.

Appendix A. Supplementary data

Supplementary material related to this article can be found, in the online version, at doi:https://doi.org/10.1016/j.jbiotec.2020.01.001.

References

Aamir, M., Singh, V.K., Meena, M., Upadhyay, R.S., Gupta, V.K., Singh, S., 2017. Structural and functional insights into WRKY3 and WRKY4 transcription factors to unravel the WRKY –DNA (W-Box) complex interaction in tomato (*Solanum lycopersicum* L.). A computational approach. Front. Plant Sci. 8, 819.

Akerfelt, M., Morimoto, R.I., Sistonen, L., 2010. Heat shock factors: integrators of cell stress, development and lifespan. Nat. Rev. Mol. Cell Biol. 11, 545–555.

Arnon, D.I., 1949. Copper enzymes in isolated chloroplast. Polyphenoxidase in beta vulgaris. Plant Physiol. 24, 1–15.

Ashraf, M., Foolad, M.R., 2007. Roles of glycinebetaine and proline in improving plant abiotic resistance. Environ. Exp. Bot. 59, 206–216.

Bates, L.S., Waldren, R.P., Teare, I.D., 1973. Rapid determination of free proline for water-stress studies. Plant Soil 39, 205–207.

Benkert, P., Kunzli, M., Schwede, T., 2009. QMEAN server for protein model quality estimation. Nucleic Acids Res. 37, W510–W514.

Berman, J., Westbrook, Z., Gilliland, G., Bhat, T.N., Weissig, H., et al., 2000. The protein data bank. Nucleic Acids Res. 28, 235–242.

Biasini, M., Bienert, S., Waterhouse, A., Arnold, K., Studer, G., Schmidt, T., Kiefer, F., Cassarino, T.G., Bertoni, M., Bordoli, L., Schwede, T., 2014. SWISS-MODEL: modelling protein tertiary and quaternary structure using evolutionary information. Nucleic Acids Res. 42, W252–W258.

Bita, C., Gerats, T., 2013. Plant tolerance to high temperature in a changing environment: scientific fundamentals and production of heat stress-tolerant crops. Front. Plant Sci. 4, 273.

Brewbaker, J.L., Kwack, B.H., 1963. The essential role of calcium ion in pollen germination and pollen tube growth. Am. J. Bot. 50, 859–865.

Castrignano, T., De Meo, P.D., Cozzetto, D., Talamo, I.G., Tramontano, A., 2006. The PMDB protein model database. Nucleic Acids Res. 34, D306–D309.

Cazalis, R., Pulido, P., Aussenac, T., Perez-Ruiz, J.M., Cejudo, F.J., 2006. Cloning and characterization of three thioredoxin h isoforms from wheat showing differential expression in seeds. J. Exp. Bot. 57, 2165–2172.

Colovos, C., Yeates, T.O., 1993. Verification of protein structures: patterns of nonbonded atomic interactions. Protein Sci. 2, 1511–1519.

Cruz de Carvalho, M.H., 2008. Drought stress and reactive oxygen species: production, scavenging and signaling. Plant Signal. Behav. 3, 156–165.

Csiszar, J., Horváth, E., Vary, Z., Galle, A., Bela, K., Brunner, S., et al., 2014. Glutathione transferase supergene family in tomato: salt stress regulated expression of representative genes from distinct GST classes in plants primed with salicylic acid. Plant Physiol. Biochem. 78, 15–26.

Das, S., Lee, D., Sillitoe, I., Dawson, N.L., Lees, J.G., Orengo, C.A., 2016. Functional classification of CATH superfamilies: a domainbased approach for protein function annotation. Bioinformatics 32, 2889.

De Boeck, H.J., Bassin, S., Verlinden, M., Zeiter, M., Hiltbrunner, E., 2015. Simulated heat waves affected alpine grassland only in combination with drought. New Phytol. 209, 531–554.

De Castro, E., Sigrist, C.J.A., Gattiker, A., Bulliard, V., Langendijk-Genevaux, P.S., Gasteiger, E., et al., 2006. ScanProsite: detection of PROSITE signature matches and ProRule-associated functional and structural residues in proteins. Nucleic Acids Res. 1, 362–365.

Deshmukh, P.S., Sairam, R.K., Shukla, D.S., 1991. Measurement of ion leakage as a screening technique for drought resistance in wheat phenotypical groups. Indian J. Plant Physiol. 34, 89–91.

Fan, Q.J., Liu, J.H., 2012. Nitric oxide is involved in dehydration/drought tolerance in *Poncirus trifoliata* seedlings through regulation of antioxidant systems and stomatal response. Plant Cell Rep. 31, 145–154.

Federico, M.L., Kaeppler, H.F., Skadsen, R.W., 2005. The complex developmental expression of a novel stress-responsive barley Ltp gene is determined by a shortened promoter sequence. Plant Mol. Biol. 57, 35–51.

Fragkostefanakis, S., Roeth, S., Schleiff, E., Scharf, K.D., 2015. Prospects of engineering thermotolerance in crops through modulation of heat stress transcription factor and heat shock protein networks. Plant Cell Environ. 38 (9), 1881–1895.

Gao, W., Bai, S., Li, Q., Gao, C., Liu, G., Li, G., Tan, F., 2013. Overexpression of *TaLEA* gene from Tamarix androssowii improves salt and drought tolerance in transgenic poplar (*Populus simonii* × *Populus nigra*). PLoS One 8, 1–7.

Gill, S.S., Hasanuzzaman, M., Nahar, K., Macovei, A., Tuteja, N., 2013. Importance of nitric oxide in cadmium stress tolerance in crop plants. Plant Physiol. Biochem. 63, 254–261.

Guo, M., Liu, J., Ma, X., Luo, D., Gong, Z., Lu, M., 2016. The plant heat stress transcription factors (HSFs): structure, regulation and function in response to abiotic stresses. Front. Plant Sci. 7, 114.

Hasan, M.A., Al-Taweel, S.K., Alamrani, H.A., Al-Naqeeb, M.A., Al-Baldawwi, M.H.K., Hamza, J.H., 2018. Anatomical and physiological traits of broad bean (*Vicia faba* L.) seedling affected by salicylic acid and salt stress. Indian J. Agric. Res. 52 (4), 362–367.

Hasanuzzaman, M., Nahar, K., Alam, M.M., Fujita, M., 2012. Exogenous nitric oxide alleviates high temperature induced oxidative stress in wheat (*Triticum aestivum* L.) seedlings by modulating the antioxidant defense and glyoxalase system. Aust. J. Crop Sci. 6, 1314–1323.

Hasanuzzaman, M., Nahar, K., Alam, M.M., Roychowdhury, R., Fujita, M., 2013. Physiological, biochemical, and molecular mechanisms of heat stress tolerance in plants. In. J. Mol. Sci. 14, 9643–9684.

Hasanuzzaman, M., Nahar, K., Hossain, M.S., Mahmud, J.A., Rahman, A., Inafuku, M., Oku, H., Fujita, M., 2017. Coordinated actions of glyoxalase and antioxidant defense systems in conferring abiotic stress tolerance in plants. Int. J. Mol. Sci. 18, 200.

Heath, R.L., Packer, L., 1968. Photoperoxidation in isolated chloroplasts. Kinetics and stoichiometry of fatty acid peroxidation. Arch. Biochem. Biophys. 125, 189–198.

Hietakangas, V., Ahlskog, J.K., Jakobsson, A.M., Hellesuo, M., Sahlberg, N.M., Holmberg, C.I., Mikhailov, A., Palvimo, J.J., Pirkkala, L., Sistonen, L., 2003. Phosphorylation of serine 303 is a prerequisite for the stress-inducible SUMO modification of heat shock factor 1. Mol. Cell. Biol. 23, 2953–2968.

Hu, B., Jin, J., Guo, A.Y., Zhang, H., Luo, J., Gao, G., 2014. GSDS 2.0: an upgraded gene feature visualization server. Bioinformatics 31, 1296–1297.

Hussain, M., Malik, M.A., Farooq, M., Khan, M.B., Akram, M., Saleem, M.F., 2009. Exogenous glycinebetaine and salicylic acid application improves water relations, allometry and quality of hybrid sunflower under water deficit conditions. J. Agron. Crop Sci. 195 (2), 98–109.

Ikeda, M., Ohme-Takagi, M., 2009. A novel group of transcriptional repressors in Arabidopsis. Plant Cell Physiol. 50, 970–975.

IPCC, 2014. Summary for policymakers. In: Field, C.B., Barros, V.R., Dokken, D.J., Mach, K.J., Mastrandrea, M.D., Bilir, T.E., Chatterjee, M., Ebi, K.L., Estrada, Y.O., Genova, R.C., Girma, B., Kissel, E.S., Levy, A.N., MacCracken, S., Mastrandrea, S., White, L.L. (Eds.), Climate Change 2014: Impacts, Adaptation, and Vulnerability. Part A: Global and Sectoral Aspects. Contribution of Working Group II to the Fifth Assessment Report of the Intergovernmental Panel on Climate Change. Cambridge University Press, pp. 1–32.

Jabs, T., Dietrich, R.A., Dangl, J.L., 1996. Initiation of runaway cell death in an Arabidopsis mutant by extracellular superoxide. Science 273, 1853–1856.

Jaeger, A.M., Pemble, C.W., Sistonen, L., Thiele, D.J., 2016. Structures of HSF2 reveal mechanisms for differential regulation of human heat-shock factors. Nat. Struct. Mol. Biol. 23 (2), 147.

Jana, S., Choudhuri, M.A., 1981. Glycolate metabolism of three submerged aquatic angiosperm during aging. Aquat. Bot. 12, 345–354.

Janda, T., Szalai, G., Tari, I., Paldi, E., 1999. Hydroponic treatment with salicylic acid decreases the effects of chilling injury in maize (*Zea mays* L.) plants. Planta. 208, 175–180.

Jiang, Y., Deyholos, M.K., 2009. Functional characterization of Arabidopsis NaCl-inducible WRKY25 and WRKY33 transcription factors in abiotic stresses. Plant Mol. Biol. 69, 91–105.

Jimenez-Quesada, M.J., Carmona, R., Lima-Cabello, E., Traverso, J.A., Castro, A.J., Claros, M.G., de Dios Alche, J., 2017. Generation of nitric oxide by olive (*Olea europaea* L.) pollen during in vitro germination and assessment of the S-nitroso-and nitro-proteomes by computational predictive methods. Nitric Oxide 68, 23–37.

Jin, J.P., Zhang, H., Kong, L., Gao, G., Luo, J.C., 2014. PlantTFDB 3.0: a portal for the functional and evolutionary study of plant transcription factors. Nucleic Acids Res. 42, D1182–D1187.

Kang, G.Z., Li, G.Z., Liu, G.Q., Xu, W., Peng, X.Q., Wang, C.Y., et al., 2013. Exogenous salicylic acid enhances wheat drought tolerance by influence on the expression of genes related to ascorbate-glutathione cycle. Biol. Plant. 57, 718–724.

Khan, M.I.R., Asgher, M., Khan, N.A., 2014. Alleviation of salt-induced photosynthesis and growth inhibition by salicylic acid involves glycinebetaine and ethylene in mungbean (*Vigna radiata* L.). Plant Physiol. Biochem. 80, 67–74.

Khan, N.A., Nazar, R., Iqbal, N., Anjum, N.A., 2012. Phytohormones and Abiotic Stress Tolerance in Plants. Springer, Berlin. https://doi.org/10.1007/978-3-642-25829-9.

Khokon, M., Okuma, E.I.J.I., Hossain, M.A., Munemasa, S., Uraji, M., Nakamura, Y., et al., 2011. Involvement of extracellular oxidative burst in salicylic acid-induced stomatal closure in Arabidopsis. Plant Cell Environ. 34, 434–443.

Kotak, S., Vierling, E., Bäumlein, H., von Koskull-Doring, P., 2007. A novel transcriptional cascade regulating expression of heat stress proteins during seed development of Arabidopsis. Plant Cell 19, 182–195.

Kreps, J.A., Wu, Y., Chang, H.S., Zhu, T., Wang, X., Harper, J.F., 2002. Transcriptome changes for Arabidopsis in response to salt, osmotic. and cold stress. Plant physiol. 130, 2129–2141.

Krzywinski, M., Schein, J., Birol, I., Connors, J., Gascoyne, R., Horsman, D., et al., 2009. Circos: an information aesthetic for comparative genomics. Genome Res. 19, 1639–1645.

Laskowski, R.A., Chistyakov, V.V., Thornton, J.M., 2005. PDBsum more: new summaries and analyses of the known 3D structures of proteins and nucleic acids. Nucleic Acids Res. 1, D266–D268.

Law, M.Y., Charles, S.A., Halliwell, B., 1983. Glutathione and ascorbic acid in spinach (*Spinacea oleracea*) chloroplast: the effect of hydrogen peroxide and paraquat. Biochem. J. 210, 899–903.

Lee, M.Y., Shin, K.H., Kim, Y.K., Suh, J.Y., Gu, Y.Y., Kim, M.R., Hur, Y.S., Son, O., Kim,

J.S., Song, E., Lee, M.S., Nam, K.H., Hwang, K.H., Sung, M.K., Kim, H.J., Chun, J.Y., Park, M., Ahn, T.I., Hong, C.B., Lee, S.H., Park, H.J., Park, J.S., Verma, D.P., Cheon, C.I., 2005. Induction of thioredoxin is required for nodule development to reduce reactive oxygen species levels in soybean roots. Plant Physiol. 139, 1881–1889.
Li, G., Peng, X., Wei, L., Kang, G., 2013. Salicylic acid increases the contents of glutathione and ascorbate and temporally regulates the related gene expression in salt-stressed wheat seedlings. Gene 529, 321–325.
Livak, K.J., Schmittgen, T.D., 2001. Analysis of relative gene expression data using real-time quantitative PCR and the $2^{-\Delta\Delta Ct}$ method. Methods 25, 402–408.
Lovell, S.C., Davis, I.W., Arendall, W.B., de Bakker, P.I., Word, J.M., Prisant, M.G., Richardson, J.S., Richardson, D.C., 2003. Structure validation by Ca geometry: phipsi and C-beta deviation. Proteins 50, 437–450.
Lowry, O.H., Rosenbrough, R.J., Farr, A.L., Randall, R.J., 1951. Protein measurement with folin- phenol reagent. J. Biol. Chem. 193, 265–275.
Ma, H., Wang, C., Yang, B., Cheng, H., Wang, Z., Mijiti, A., et al., 2015. CarHSFB2, a Class B heat shock transcription factor, is involved in different developmental processes and various stress responses in chickpea (*Cicer arietinum* L.). Plant Mol. Biol. Rep. 34, 1–14.
Macindoe, G., Mavridis, L., Venkatraman, V., Devignes, M., Ritchie, D., 2010. Hex Server: an FFT-based protein docking server powered by graphic processors. Nucleic Acids Res. 38, W445–W449.
Madej, T., Lanczycki, C.J., Zhang, D., Thiessen, P.A., Geer, R.C., Marchler-Bauer, A., Bryant, S.H., 2014. MMDB and VAST+: tracking structural similarities between macromolecular complexes. Nucleic Acids Res. 42, D297–D303.
Manjunatha, G., Lokesh, V., Neelwarne, B., 2010. Nitric oxide in fruit ripening: trends and opportunities. Biotechnol. Adv. 28, 489–499.
Antony, Maria, Dhivyan, J.E., Anoop, M.N., 2012. Virtual screening and lead optimisation to identify novel inhibitors for HDAC-8. Biomolecules 2793.
McKersie, B.D., Hoekstra, F., Krieg, K., 1990. Differences in the susceptibility of plant membrane lipids to peroxidation. Biochim. Biophys. Acta-Bio. 1030, 119–126.
Meena, M., Aamir, M., Kumar, V., Swapnil, P., Upadhyay, R.S., 2018. Evaluation of morpho-physiological growth parameters of tomato in response to Cd induced toxicity and characterization of metal sensitive NRAMP3 transporter protein. Environ. Exper. Bot. 30, 144–167.
Misra, H.P., Fridovich, I., 1972. The role of superoxide anion in the autooxidation of epinephrine and a simple assay for superoxide dismutase. J. Biol. Chem. 247, 3170–3175.
Mittler, R., 2020. ROS are good. Trends Plant Sci. 22, 11–19.
Miura, K., Tada, Y., 2014. Regulation of water, salinity, and cold stress responses by salicylic acid. Fron Plant Sci. 5, 4.
Nakano, Y., Asada, K., 1981. Hydrogen peroxide is scavenged by ascorbate specific peroxides in spinach chloroplast. Plant Cell Physiol. 22, 867–880.
Nazar, R., Umar, S., Khan, N.A., 2015. Exogenous salicylic acid improves photosynthesis and growth through increase in ascorbate-glutathione metabolism and S assimilation in mustard under salt stress. Plant Signal. Behav. 10, e1003751.
Neudegger, T., Verghese, J., Hayer-Hartl, M., Hartl, F.U., Bracher, A., 2016. Structure of human heat-shock transcription factor 1 in complex with DNA. Nat. Struct. Mol. Biol. 23, 140.
Owens, C.W.I., Belcher, R.V., 1965. A colorimetric micro-method for the determination of glutathione. Biochem. J. 94, 705–711.
Porra, R.J., Thompson, W.A., Kriedemann, P.E., 1989. Determination of accurate extinction coefficients and simultaneous equations for assaying chlorophylls a and b extracted with four different solvents: verification of the concentration of chlorophyll standards by atomic absorption spectroscopy. Biochim. Biophys. Acta-Bio. 975, 384–394.
Rai, K.K., Rai, N., Rai, S.P., 2017. Downregulation of γ ECS gene affects antioxidant activity and free radical scavenging system during pod development and maturation in *Lablab purpureus* L. Biocatal. J. Agric. Biotechnol. Sustain. Dev. 11, 192–200.
Rai, K.K., Rai, N., Rai, S.P., 2018a. Investigating the impact of high temperature on growth and yield of *Lablab purpureus* L. Inbred lines using integrated phenotypical, physiological, biochemical and molecular approaches. Indian J. Plant Physiol. 23, 209–226.
Rai, K.K., Rai, N., Rai, S.P., 2018b. Salicylic acid and nitric oxide alleviate high temperature induced oxidative damage in *Lablab purpureus* L plants by regulating biophysical processes and DNA methylation. Plant Physiol. Biochem. 128, 72–88.
Rai, K.K., Rai, N., Rai, S.P., 2018c. Response of *Lablab purpureus* L. To high temperature stress and role of exogenous protectants in mitigating high temperature induced oxidative damages. Mol. Biol. Rep. 45, 1375–1395.
Rai, K.K., Rai, N., Rai, S.P., 2018d. Recent advancement in modern genomic tools for adaptation of *Lablab purpureus* L to biotic and abiotic stresses: present mechanisms and future adaptations. Acta Physiol. Plant. 40, 164.
Rai, N., Rai, K.K., Tiwari, G., Singh, P.K., 2015. Changes in free radical generation, metabolites and antioxidant defense machinery in hyacinth bean (*Lablab purpureus* L.) in response to high temperature stress. Acta Physiol. Plant. 37, 46.
Rai, N., Rai, K.K., Venkataravanappa, V., Saha, S., 2016. Molecular approach coupled with biochemical attributes to elucidate the presence of DYMV in leaf samples of *Lablab purpureus* L. Genotypes. Appl. Biochem. Biotechnol. 178, 876–890.
Ritchie, D.W., 2003. Evaluation of protein docking predictions using Hex 3.1 in CAPRI rounds 1 and 2. Proteins 52, 98–106.
Rodriguez Sanchez, E., Rubio-Wilhelmi, M.M., Cervilla, L.M., Blasco, B., Rios, J.J., Rosales, M.A., Romero, L., Ruiz, J.M., 2010. Genotypic differences in some physiological parameters symptomatic for oxidative stress under moderate drought in tomato plants. Plant Sci. 178, 30–40.
Salamov, A.A., Solovyev, V.V., 2000. Ab initio gene finding in Drosophila genomic DNA. Genome Res. 10 (4), 516–522.
Saruhan, N., Saglam, A., Kadioglu, A., 2012. Salicylic acid pre-treatment induces drought tolerance and delays leaf rolling by inducing antioxidant systems in maize genotypes. Acta Physiol. Plant. 34, 97–106.
Scharf, K.D., Berberich, T., Ebersberger, I., Nover, L., 2012. The plant heat stress transcription factor (Hsf) family: structure, function and evolution. Biochim. Biophys. Acta-Gene Regul. Mech. 1819, 104–119.
Shah, K., Kumar, R.G., Verma, S., Dubey, R.S., 2001. Effect of cadmium on lipid peroxidation, superoxide anion generation and activities of antioxidant enzymes in growing rice seedlings. Plant Sci. 161, 1135–1144.
Sillitoe, I., Lewis, T.E., Cuff, A., Das, S., Ashford, P., Dawson, N.L., et al., 2015. CATH: comprehensive structural and functional annotations for genome sequences. Nucleic Acids Res. 43, D376–D381.
Sun, M.G., Kim, P.M., 2011. Evolution of biological interaction networks: from models to real data. Genome Biol. 12, 235.
Supek, F., Bosnjak, M., Skunca, N., Smuc, T., 2011. REVIGO summarizes and visualizes long lists of gene ontology terms. PLoS One 6, e21800.
Szklarczyk, D., Franceschini, A., Wyder, S., Forslund, K., Heller, D., HuertaCepas, J., et al., 2015. STRING v10: protein–protein interaction networks, integrated over the tree of life. Nucleic Acids Res. 43, D447–D452.
Tada, Y., Spoel, S.H., Pajerowska-Mukhtar, K., Mou, Z., Song, J., Wang, C., Zuo, J., Dong, X., 2008. Plant immunity requires conformational charges of NPR1 via S-nitrosylation and thioredoxins. Science 321, 952–956.
Tamura, K., Stecher, G., Peterson, D., Filipski, A., Kumar, S., 2013. MEGA6: molecular evolutionary genetics analysis version 6.0. Mol. Biol. Evol. 30, 2725–2729.
Thordal-Christensen, H., Zhang, Z., Wei, Y., Collinge, D.B., 1997. Subcellular localization of H_2O_2 in plants. H_2O_2 accumulation in papillae and hypersensitive response during the barley—powdery mildew interaction. Plant J. 11 (6), 1187–1194.
Ticha, T., Cincalova, L., Kopecny, D., Sedlarova, M., Kopecna, M., Luhova, L., Petrivalsky, M., 2017. Characterization of S-nitrosoglutathione reductase from Brassica and Lactuca spp. and its modulation during plant development. Nitric Oxide 68, 68–76.
Vatansever, R., Filiz, E., Ozyigit, I.I., 2016. In silico analysis of Mn transporters (NRAMP1) in various plant species. Mol. Biol. Rep. 43, 151–163.
Vihervaara, A., Sergelius, C., Vasara, J., Blom, M.A.H., Elsing, A.N., Roos-Mattjus, P., et al., 2013. Transcriptional response to stress in the dynamic chromatin environment of cycling and mitotic cells. Proc. Natl. Acad. Sci. U.S.A. 110, E3388–E3397.
Wang, C., Yang, C., Gao, C., Wang, Y., 2009. Cloning and expression analysis of 14 lipid transfer protein genes from *Tamarix hispida* responding to different abiotic stresses. Tree Physiol. 29, 1607–1619.
Wang, J., Sun, N., Deng, T., Zhang, L., Zuo, K., 2014. Genome-wide cloning, identification, classification and functional analysis of cotton heat shock transcription factors in cotton (*Gossypium hirsutum*). BMC Genomics 15, 961.
Wang, J., Yu, N., Mu, G., Shinwari, K.I., Shen, Z., Zheng, L., 2017. Screening for Cd-safe cultivars of Chinese cabbage and a preliminary study on the mechanisms of Cd accumulation. Int. J. Environ. Res. Public Health 14, 395.
Wang, L.J., Fan, L., Loescher, W., Duan, W., Liu, G.J., Cheng, J.S., et al., 2010. Salicylic acid alleviates decreases in photosynthesis under heat stress and accelerates recovery in grapevine leaves. BMC Plant Biol. 10, 34.
Wang, L.J., Li, S.H., 2006. Salicylic acid-induced heat or cold tolerance in relation to $Ca2^{+}$ homeostasis and antioxidant systems in young grape plants. Plant Sci. 170, 685–694.
Wang, P., Du, Y., Hou, Y.J., Zhao, Y., Hsu, C.C., Yuan, F., Zhu, X., Tao, W.A., Song, C.P., Zhu, J.K., 2015. Nitric oxide negatively regulates abscisic acid signaling in guard cells by S-nitrosylation of OST1. Proc. Natl. Acad. Sci. U.S.A. 112 (2), 613–618.
Wang, W., Vinocur, B., Shoseyov, O., Altman, A., 2004a. Role of plant heatshock proteins and molecular chaperones in the abiotic stress response. Trend Plant Sci. 9, 244–252.
Wang, Z.Y., Ge, Y., Scott, M., Spangenberg, G., 2004b. Viability and longevity of pollen from transgenic and nontransgenic tall fescue (*Festuca arundinacea*) (Poaceae) plants. Am. J. Bot. 91, 523–530.
Wiederstein, M., Sippl, M.J., 2007. ProSA-web: interactive web service for the recognition of errors in three-dimensional structures of proteins. Nucleic Acids Res. 35, W407–W410.
Willard, L., Ranjan, A., Zhang, H., Monzavi, H., Boyko, R.F., Sykes, B.D., Wishart, D.S., 2003. VADAR: a web server for quantitative evaluation of protein structure quality. Nucleic Acids Res. 31, 3316–3319.
Xiao, B., Huang, Y., Tang, N., Xiong, L., 2007. Over-expression of a LEA gene in rice improves drought resistance under the weld conditions. Theor. Appl. Genet. 115, 35–46.
Xu, D., Zhang, Y., 2011. Improving the physical realism and structural accuracy of protein models by a two-step atomic-level energy minimization. Biophys. J. 101, 2525–2534.
Xu, Q., Hu, Y., Kleindienst, R., Wick, G., 1997. Nitric oxide induces heat-shock protein 70 expression in vascular smooth muscle cells via activation of heat shock factor 1. Clin. Investig. 100, 1089–1097.
Yao, L.M., Wang, B., Cheng, L.J., Wu, T.L., 2013. Identification of key drought stress-related genes in the hyacinth bean. PLoS One 8, e58108.
Yu, C.S., Cheng, C.W., Su, W.C., Chnag, K.C., Huang, S.W., Hwang, J.K., et al., 2014. CELLO2GO: a web server for protein subcellular localization prediction with functional gene ontology annotation. PLoS One 9, e99368.
Zandalinas, S.I., Rivero, R.M., Martínez, V., Gómez-Cadenas, A., Arbona, V., 2016. Tolerance of citrus plants to the combination of high temperatures and drought is associated to the increase in transpiration modulated by a reduction in abscisic acid levels. BMC Plant Biol. 16, 105.
Zhang, X.W., Zhang, M., Wang, Q.H., Qiu, X.K., Hu, G.Q., Dong, Y.J., 2011. Effect of exogenous nitric oxide on physiological characteristic of peanut under iron deficient stress. J. Plant Nutr. Fert. 17, 665–673.
Zhang, Y., Xu, S., Yang, S., Chen, Y., 2015. Salicylic acid alleviates cadmium induced inhibition of growth and photosynthesis through upregulating antioxidant defence system in two melon cultivars (*Cucumis melo* L.). Protoplasma 252, 911–924.